DOC.20030709.0001

OCRWM	MODEL COVER SHEET	1. QA: QA Page 1 of 68

2. Type of Mathematical Model

☒ Process Model ☐ Abstraction Model ☐ System Model

Describe Intended Use of Model

The purpose of this Model Report is to document the predictions and analyses performed using the Seepage Model for Performance Assessment (SMPA) for both the Topopah Spring middle nonlithophysal (Tptpmn) and lower lithophysal (Tptpll) lithostratigraphic units at Yucca Mountain, Nevada. Look-up tables of seepage flow rates into a drift (and their uncertainty) are generated by performing numerical simulations with the SMPA for many combinations of the three most important seepage-relevant parameters—the fracture permeability, the capillary-strength parameter 1/α, and percolation flux. Moreover, multiple realizations of the underlying stochastic permeability field are conducted. Selected sensitivity studies are performed, including the effects of an alternative drift geometry representing a partially collapsed drift from an independent drift-degradation analysis (BSC 2001 [156304]). The intended purpose of the SMPA is to provide results of drift-scale seepage rates under a series of parameters and scenarios, in support of the Total System Performance Assessment for License Application (TSPA-LA).

3. Title

Seepage Model for PA Including Drift Collapse

4. DI (Including Rev. No. and Change No., if applicable):

MDL-NBS-HS-000002 REV02

5. Total Attachments	6. Attachment Numbers - No. of Pages in Each
4	I-16, II-2, III-2, IV-2

	Printed Name	Signature	Date
7. Originator	C.F. Tsang	SIGNATURE ON FILE	7/3/03
8. CSO	M. Zhu	SIGNATURE ON FILE	7-3-03
9. Checker	G. Su	SIGNATURE ON FILE	7/3/03
10. QER	K. Gilkeson	SIGNATURE ON FILE	7/3/03
11. Responsible Manager/Lead	J.S.Y. Wang/S. Finsterle	SIGNATURE ON FILE	7/3/03
12. Responsible Manager	P. Dixon	SIGNATURE ON FILE	7/3-03

13. Remarks

Block 7. Additional contributors to this Model Report are G. Li (all sections), S. Finsterle (Section 7), and J. Ramqvist (Section 6.7).

Technical Error Report (TER) log number addressed in this Model Report:
TER-02-0078

MODEL REVISION RECORD

2. Model Title:

Seepage Model for PA Including Drift Collapse

3. DI (including Rev. No. and Change No., if applicable):

MDL-NBS-HS-000002 REV02

4. Revision/Change No.	5. Description of Revision/Change
00	Initial Issue
01	The Seepage Model for PA Including Drift Collapse has been revised using updated parameter sets from the Seepage Calibration Model (MDL-NBS-HS-000004 REV01, CRWMS M&O 2001 [153045]). The entire model documentation was revised according to AP-3.10Q, Rev 2, ICN 3, Step 5.9)2); the changes were too extensive to use revision tracking of individual modifications.
REV02	The entire model documentation was revised using updated parameter sets from the Seepage Calibration Model (MDL-NBS-HS-000004 REV02, BSC 2003 [162267]). Side bars are not used because the changes were too extensive to use Step 5.9d)1) per AP-SIII.10Q, Rev. 1/ICN 2.

CONTENTS

CONTENTS (Continued)

FIGURES

FIGURES (Continued)

TABLES

INTENTIONALLY LEFT BLANK

ACRONYMS

2-D	two-dimensions, two-dimensional
3-D	three-dimensions, three-dimensional
ACC	Accession Number
AP	Administrative Procedure (DOE)
BSC	Bechtel SAIC Company
CRWMS	Civilian Radioactive Waste Management System
DFNM	discrete fracture network model
DIRS	Document Input Reference System
DOE	Department of Energy
DTN	Data Tracking Number
EBS	Engineered Barrier System
ECRB	Enhanced Characterization of Repository Block
ESF	Exploratory Studies Facility
FEP	features, events, and processes
ID	identification number
LA	License Application
LBNL	Lawrence Berkeley National Laboratory
m	meter
min	minute
mL	milliliter
mm	millimeter
M&O	Management and Operating Contractor
NRC	Nuclear Regulatory Commission
OCRWM	Office of Civilian Radioactive Waste Management
Pa	pascal (as a unit of measure)
PA	Performance Assessment
PTn	Paintbrush nonwelded unit
QA	Quality Assurance

ACRONYMS (Continued)

s	second
SCM	Seepage Calibration Model
SMPA	Seepage Model for Performance Assessment
SNs	Scientific Notebooks
Std. Dev.	standard deviation
STN	Software Tracking Number
TBV	to be verified
TDMS	Technical Data Management System
TER	Technical Error Report
TH	thermal-hydrological
THC	thermal-hydrological-chemical
THM	thermal-hydrological-mechanical
TM	thermal-mechanical
Tptpll	lower lithophysal zone of Topopah Spring Tuff
Tptpmn	middle nonlithophysal zone of Topopah Spring Tuff
TSPA-LA	Total System Performance Assessment for License Application
TSw	Topopah Spring welded unit
TWP	Technical Work Plan
U.S.	United States
UZ	unsaturated zone
UZ Model	Unsaturated Zone Flow and Transport Model
wp	waste package
YMP	Yucca Mountain Project
YMRP	*Yucca Mountain Review Plan, Information Only*

1. PURPOSE

The purpose of this Model Report is to document the predictions and analyses performed using the Seepage Model for Performance Assessment (SMPA) for both the Topopah Spring middle nonlithophysal (Tptpmn) and lower lithophysal (Tptpll) lithostratigraphic units at Yucca Mountain, Nevada. Look-up tables of seepage flow rates into a drift (and their uncertainty) are generated by performing numerical simulations with the SMPA for many combinations of the three most important seepage-relevant parameters—the fracture permeability, the capillary-strength parameter $1/\alpha$, and percolation flux. Moreover, multiple realizations of the underlying stochastic permeability field are conducted. Selected sensitivity studies are performed, including the effects of an alternative drift geometry representing a partially collapsed drift from an independent drift-degradation analysis (BSC 2001 [156304]). The intended purpose of the SMPA is to provide results of drift-scale seepage rates under a series of parameters and scenarios, in support of the Total System Performance Assessment for License Application (TSPA-LA).

The SMPA serves as a link between the Seepage Calibration Model (SCM; BSC 2003 [162267]) and the upcoming revision of Seepage Abstraction (CRWMS M&O 2001 [154291]). The SCM evaluates available field data from air-injection and liquid-release tests performed in niches and the Enhanced Characterization of Repository Block (ECRB) Cross Drift, uses an equivalent fracture continuum model, and calibrates parameter values to reproduce the observed seepage-rate data. The SMPA then adopts the same conceptual framework from the SCM to systematically evaluate seepage into waste emplacement drifts by performing flow simulations with multiple realizations of the permeability field around the drift, using a wide range of key parameters. Sensitivity analyses are performed, in which the three-dimensional (3-D) flow of water in the fractured host rock and potential seepage into emplacement drifts are simulated for a variety of hydrogeologic conditions. In particular, a disturbed-drift seepage case evaluates the sensitivity of seepage results to the effects of partial drift collapse as well as of ground support using rock bolts. However, the effects of potential igneous disruptive events and enhanced drift degradation resulting from the loss of rock cohesive strength are not included in the present Model Report. They will be addressed in the upcoming revision of *Abstraction of Drift Seepage* (CRWMS M&O 2001 [154291]) described in the *Technical Work Plan (TWP) for: Performance Assessment Unsaturated Zone* (BSC 2002 [160819], Section 1.13.5). The main results from the SMPA are in the form of calculated seepage rates as a function of fracture medium permeability k_{FC}, the van Genuchten $1/\alpha$ parameter, and percolation flux Q_p. The seepage rates are presented as mean values and standard deviations over statistical realizations at each combination of the parameter set. These are then fed into Seepage Abstraction (CRWMS M&O 2001 [154291]) to be eventually used for TSPA-LA.

The work scope of this Model Report is based on the TWP (BSC 2002 [160819], Section 1.13.4). It is carried out through the following steps:

(1) Develop the SMPA, which is a process model simulating unsaturated flow and seepage into a segment of a waste emplacement drift.

(2) Review the parameter sets covering both Tptpmn and Tptpll units developed in the SCM and the percolation flux predictions from the Unsaturated Zone (UZ) Site Scale Flow and Transport Model (UZ Model) to derive ranges of permeability as well as van Genuchten capillary-strength parameters and percolation fluxes to be examined by the SMPA. The results from coupled thermal-hydro-chemical and coupled thermal-hydro-mechanical models are to be considered in the selection of parameter ranges.

(3) Design a set of simulations for evaluating drift seepage, using a model structure consistent with that of the SCM.

(4) Perform multiple realizations of the heterogeneous permeability field and subsequently simulate drift seepage using the SMPA.

(5) Review information from existing drift collapse models provided by the Yucca Mountain Project (YMP) Engineered Barrier System (EBS) department and develop a representation of the geometry of a partially collapsed drift.

(6) Perform simulations using the degraded drift profiles.

(7) Use the SMPA to evaluate the impact of the presence of a rock bolt used for ground support.

(8) Provide the basis for screening arguments concerning certain seepage-related features, events, and processes (FEPs); see Section 6.2.1.

The primary caveats and limitations on the results from the SMPA are that its basis is limited to the current repository design, available site data, and upstream models. This includes the drift configuration defined by the current design and analysis, available hydrological properties data from the site, limitations reported in Model Reports that directly support this Model Report, and consideration of seepage under ambient conditions only. Thus, thermal-hydrological and thermal-hydrological-mechanical effects are not considered in this Model Report. Some discussions of these effects on long-term hydrological properties, especially those resulting from irreversible processes, are discussed in Section 6.7. Furthermore, the model is based on and consistent with the conceptualization of the SCM; it therefore considers the same features and seepage mechanisms. For example, the seepage calculations do not include water dripping as a result of condensate accumulation on the drift surface or other in-drift moisture redistributing processes.

Note that the purpose of this Model Report is to document the predictions from the SMPA and not to draw conclusions about final PA predictions. It forms the link between field data, calibrated-model parameters, and the PA effort. Developed results of the SMPA are summarized in the following Output-DTNs: LB0304SMDCREV2.001, LB0304SMDCREV2.002, LB0304SMDCREV2.003, and LB0304SMDCREV2.004 (see Attachment I).

The technical scope, content, and management of this Model Report are controlled by the TWP (BSC 2002 [160819]). There were no deviations from the TWP.

2. QUALITY ASSURANCE

Development of this Model Report and the supporting modeling activities have been determined to be subject to the Yucca Mountain Project's quality assurance (QA) program as indicated in *Technical Work Plan for: Performance Assessment Unsaturated Zone,* TWP-NBS-HS-000003 REV 02 (BSC 2002 [160819], Section 8.2, Work Package AUZM09). Approved QA procedures identified in the TWP (BSC 2002 [160819], Section 4) have been used to conduct and document the activities described in this model report. The TWP also identifies the methods used to control the electronic management of data (BSC 2002 [160819], Section 8.4, Work Package AUZM09) during the modeling and documentation activities.

This Model Report examines the properties of a natural barrier that are important to the demonstration of compliance with the postclosure performance objectives prescribed in 10 CFR 63 [156605], Section 63.113. Natural barriers are classified as a "Quality Level – 1" with regard to importance to waste isolation, as defined in AP-2.22Q, *Classification Criteria and Maintenance of the Monitored Geologic Repository Q-List*. The report contributes to the analysis and modeling data used to support performance assessment; the conclusions do not directly impact engineered features important to preclosure safety, as defined in AP-2.22Q.

INTENTIONALLY LEFT BLANK

3. USE OF SOFTWARE

The software programs used in this study are listed in Table 3-1. These are appropriate for the intended application and were used only within the range of validation. They were obtained from Software Configuration Management and qualified under AP-SI.1Q, *Software Management.* They were all run in the versions of operating system as listed in the Software Baseline Report.

Table 3-1. Qualified Software Programs Used in This Report

Software Name	Version	Software Tracking Number	Reference
iTOUGH2	5.0	10003-5.0-00	LBNL 2002 [160106]
GSLIB	V1.0SISIM1.204	10397-1.0SISIMV1.204-00	LBNL 2000 [153100]
MoveMesh	1.0	10358-1.0-00	LBNL 2000 [152824]
AddBound	1.0	10357-1.0-00	LBNL 2000 [152823]
Perm2Mesh	1.0	10359-1.0-00	LBNL 2000 [152826]
CutDrift	1.0	10375-1.0-00	LBNL 2000 [152816]
TOUGH2	1.4	10007-1.4-01	LBNL 2000 [146496]
EXT	1.0	10047-1.0-00	LBNL 1999 [134141]
CutNiche	1.3	10402-1.3-00	LBNL 2000 [152828]

The use of the software programs identified in Table 3-1 is documented in Section 6 and in the supporting Scientific Notebooks (SNs, Table 6-1). A summary description of the programs and their use is given below.

The program iTOUGH2 V5.0 (LBNL 2002 [160106]) has—among other features—the capability to perform extensive parameter sensitivity analyses based on the TOUGH2 simulator (BSC 2002 [161067], Section 1.2). The program is used in this Model Report for predicting seepage rates.

The GSLIB V1.0SISIM1.204 (LBNL 2000 [153100]) generates 3-D, spatially correlated random fields by means of sequential indicator simulations. It is used in this Model Report to generate spatially correlated fields of log-permeability modifiers. The TOUGH2 V1.4 (LBNL 2000 [146496]) is used for a fine-grid analysis of the rock bolt problem.

The following utility programs support the generation of computational meshes. The software program MoveMesh V1.0 (LBNL 2000 [152824]) adds a constant to the coordinates of a mesh file translating the coordinate system. This allows the relabelling of a subdomain of the mesh file to be used for detailed calculations. The software program AddBound V1.0 (LBNL 2000 [152823]) adds boundary elements to a mesh file. The software program Perm2Mesh V1.0 (LBNL 2000 [152826]) maps a field of log-permeability modifiers onto a mesh file. The software program CutDrift V1.0 (LBNL 2000 [152816]) cuts a drift portion with diameter of 5.5 m from the mesh domain. The software program CutNiche V1.3 (LBNL 2000 [152828]) cuts a rock-fall volume above the drift in the mesh domain. The software program EXT V1.0 (LBNL 1999 [134141]) generates 3D Tecplot formatted data from iTOUGH2 output files. Table 3-2

summarizes the commercial, off-the-shelf software used in support of this Model Report. These software products are exempt from qualification under AP-SI.1Q.

Table 3-2. Software Products Exempt from Qualification under AP-SI.1Q

Software Name	Version	Platform Information	Used for…
MS EXCEL	2000 (9.0.3821 SR-1)	PC, Windows 98 PC, Windows 2000 Professional	Data reduction, computation, graphical representation of output in all figures in Section 6.6, and in Table 7.1. Details given in Attachments II–IV.
Tecplot	8.0-0-6, 9.0-0-9 and 9.0-3-0	PC, Windows 98 PC, Windows 2000 Professional	Technical 3D figures (Figures 6.1, 6.4–6.8, 6.14, 6.16, 6.18, and 6.20)

4. INPUTS

4.1 DATA AND PARAMETERS

This Model Report presents calculated potential seepage rates over ranges of parameter values. The PA abstraction and evaluation will be presented in a separate Model Report, in which probability weighting factors will be discussed for parameter values and scenarios that are appropriate to the repository horizon at Yucca Mountain (see the upcoming revision of the Model Report, *Abstraction of Drift Seepage* CRWMS M&O (2001 [154291]). Hence, for this Model Report, while some data are used as direct input to model calculations, other data have been used mainly to establish the limits of the parameter ranges to be used. Also, information on rock-fall scenarios is taken to design special cases to study their potential impact on the seepage results. Table 4-1 through 4-3 present direct-input data, and Table 4-4 presents data used to establish parameter ranges and scenarios used in the current Model Report. Discussions of parameter ranges, scenarios, and uncertainties are given in Section 6.

First, the hydrologic parameters used as direct input are the van Genuchten parameter m, residual liquid saturation S_{lr} in the fracture continuum, and satiated saturation S_{ls}. These values and their sources are given in Table 4-1.

Table 4-1. Hydrogeologic Input Parameters

Description	Input Source	Value	Units
Fracture Properties for Tptpmn Unit, tsw34			
van Genuchten Parameter, m	LB997141233129.001 [104055]	0.608	[dimensionless]
Residual Liquid Saturation, S_{lr}	LB997141233129.001 [104055]	0.01	[dimensionless]
Satiated Saturation, S_{ls}	LB997141233129.001 [104055]	1.00	[dimensionless]
Fracture Properties for Tptpll Unit, tsw35			
van Genuchten Parameter, m	LB997141233129.001 [104055]	0.611	[dimensionless]
Residual Liquid Saturation, S_{lr}	LB997141233129.001 [104055]	0.01	[dimensionless]
Satiated Saturation, S_{ls}	LB997141233129.001 [104055]	1.00	[dimensionless]

Note that the parameter values for Tptpmn and Tptpll are the same except for the m parameter which is within 0.5% of each other. Geometric parameters used in the present Model Report are given in Table 4-2.

Table 4-2. Geometric Parameter Used

Description	Input Source	Value	Units
Emplacement Drift Diameter	800-IED-EBS0-00200-000-00A (BSC 2002 [160798])	5.5	m
Average Waste Package Length (average for 44-BWR and 24-BWR packages)	800-IED-EBS0-00100-000-00A (BSC 2002 [160317])	5.1	m

In Section 6.7, a sensitivity study of the thermal-hydrological-mechanical (THM) effect on seepage is conducted. Input data required for this study are listed in Table 4-3.

Table 4-3. Parameters Used in THM Study

Description	Input Source	Value/Results
van Genuchten Parameter, $1/\alpha$	LB0302SCMREV02.002 [162273]	604.3 Pa (Table 14 of BSC 2003 [162267])
Fracture Permeability Field	LB0304DRSCLTHM.001 [163703]	Figure 6.5.1-1, Figure 6.5.4-3 (d), and Figure 6.5.4-4 (d) of BSC 2003 [163501]

Information and data used in this report for establishing parameter ranges are given in Table 4-4. The appropriateness of the data is discussed in Section 6.3.

Table 4-4. Data and Information Used in This Model Report for Establishing Parameter Ranges

Description	Input Source	Comments
Results from Seepage Calibration Model: k_{FC}, $1/\alpha$	DTN: LB0302SCMREV02.002 [162273]	Statistics of post-excavation air permeabilities and calibrated $1/\alpha$ parameter for niches and systematic testing boreholes in both Tptpmn and Tptpll units.
Air-Permeability Data: k_{FC}	DTN: LB0012AIRKTEST.001 [154586]	Pre-excavation air-permeability data from Niche 1620 in the Tptpll unit (also referred to as Niche 5).
	DTN: LB980901233124.101 [136593]	Pre-excavation air-permeability data from Niches 3107 (Niche 3) and 4788 (Niche 4) in the Tptpmn unit.
	DTN: LB0011AIRKTEST.001 [153155]	Pre-excavation air-permeability data from Niche 3650 (Niche 2) and 3566 (Niche 1) in the Tptpmn unit.
	DTN: LB0205REVUZPRP.001 [159525]	Air permeability analysis.
Flow Field Simulations for Infiltration Scenarios: Q_p	DTN: LB0302PTNTSW9I.001 [162277]	Present-day, monsoon, and glacial transition low-, median-, and high-infiltration flow fields from UZ Model. Fluxes are given at the PTn/TSw interface.
Degraded Drift Profiles	DTN: MO0109RDDAAMRR.003 [156306]	Degraded drift profiles for Tptpmn and Tptpll units at worst and 75 percentile cases

NOTE: These data are used to establish parameter ranges and are not direct input. They are designated as reference only.

In addition to data in Table 4-4 used to establish parameter ranges, information on rock bolt length and annulus thickness given by BSC (2001 [155187], Section 6.5.1.2.2 and Table 4-10) is used as corroborative data to help in designing a case studied in Section 6.5.

4.2 CRITERIA

The general requirements to be satisfied by the TSPA are stated in 10 CFR 63 [156605], Section 63.114. Technical requirements to be satisfied by the TSPA are identified in the Yucca Mountain *Project Requirements Document* (Canori and Leitner 2003 [161770]). The acceptance criteria that will be used by the Nuclear Regulatory Commission (NRC) to determine whether the technical requirements have been met are identified in *Yucca Mountain Review Plan, Information Only* (YMRP; NRC 2003 [162418]). Pertinent requirements and criteria for this Model Report are summarized in Table 4-5 and described below.

Table 4-5. Project Requirements and YMRP Acceptance Criteria Applicable to This Model Report

Requirement Number[a]	Requirement Title[a]	10 CFR 63 Link	YMRP Acceptance Criteria[b]
PRD-002/T-015	Requirements for Performance Assessment	10 CFR 63.114 [156605]	Criteria 1 to 4 for *Quantity and Chemistry of Water Contacting Waste Packages and Waste Forms apply to 10 CFR 63.114 (a–c)*.
PRD-002/T-016	Requirements for Multiple Barriers	10 CFR 63.115 [156605]	Criteria 1 to 3 for *System Description and Demonstration of Multiple Barriers apply to 10 CFR 63.115 (a, b)*

NOTE: [a] from Canori and Leitner (2003 [161770])
[b] from NRC (2003 [162418], Sections 2.2.1.3.3.3 and 2.2.1.1.3)

The acceptance criteria identified in Section 2.2.1.3.3.3 of the YMRP (NRC 2003 [162418]) are given below. That these criteria are met by the present Model Report is discussed in Section 8.

- Acceptance Criterion 1, *System Description and Model Integration Are Adequate*:

  The physics of the seepage phenomenon is to be adequately incorporated into the SMPA.

- Acceptance Criterion 2, *Data Are Sufficient for Model Justification*:

  Ranges of hydrological values used in the SMPA are to be adequately justified and described.

- Acceptance Criterion 3, *Data Uncertainty Is Characterized and Propagated through the Model Abstraction*

  The parameters and their ranges used in simulations in the SMPA are to cover data uncertainties and variabilities.

- Acceptance Criterion 4, *Model Uncertainty Is Characterized and Propagated through the Model Abstraction*:

  Model uncertainty is to be characterized in the SMPA and adequately discussed and propagated through the Model Abstraction.

The acceptance criteria identified in Section 2.2.1.1.3 of the YMRP (NRC 2003 [162418] are given below. That these criteria are met by the present Model Report is discussed in Section 8.

- Acceptance Criterion 1, *Identification of Barriers is Adequate:*

  Barriers are to be adequately identified in the SMPA and linked to their capability.

- Acceptance Criterion 2, *Description of Barrier Capability to Isolate Waste is Acceptable:*

  The capability of the barrier to prevent or substantially reduce the rate of movement of water is to be described in the SMPA, including the uncertainty associated with the barrier's capability.

- Acceptance Criterion 3, *Technical Basis for Barrier Capability is Adequately Presented:*

  The technical basis for assertions of barrier capability is to be adequately discussed in the SMPA.

Note that the above criteria are updated from those listed in the TWP (BSC 2002 [160819], Table 3.1) to be consistent with the revised YMRP.

4.3 CODES AND STANDARDS

No other standards or code requirements than those referenced in Section 4.2 apply to this modeling activity.

5. ASSUMPTIONS

The SMPA is described in detail in Section 6. One assumption is used.

Assumption: the calculated worst-case and 75 percentile-case drift degradation profiles, presented in Figures 39 and 40, Table 43, (Seismic Level 3, for the Tptpmn and Tptpll units) of the report BSC (2001 [156304]), used in Section 6.4 of the current Model Report, are assumed to be appropriate for the objectives of this study.

Rationale: these degradation profiles were specifically developed for the Tptpmn and Tptpll units at Yucca Mountain, and they were the best information to refer to at the time of conducting these calculations.

Discussion: the EBS Department is conducting degradation analysis, under *Technical Work Plan for: Engineered Barrier System Department Modeling and Testing FY03 Work Activities* (BSC 2003 [163840], Section 1.2.3), involving the following activities.

- Conduct a thermal-mechanical (TM) assessment of the repository block at Yucca Mountain to determine thermal stress inputs to the drift degradation models.
- Conduct a fracture degradation assessment to account for long-term strength degradation. This assessment provides strength degradation inputs to the drift degradation models.
- Develop a drift degradation structural model for nonlithophysal rock that includes thermal and seismic loading.
- Develop a drift degradation lithophysal model that includes thermal and seismic loading.

The ongoing EBS analysis may generate additional profiles beyond the ones used in Section 6.4. Confirmation is needed when new profiles are established.

INTENTIONALLY LEFT BLANK

6. MODEL DISCUSSION

6.1 MODEL OBJECTIVES

The objectives of the SMPA are to calculate potential drift seepage under long-term, steady-state conditions for a range of percolation-flux values at the depth of the drift, as a function of the fracture continuum permeability and van Genuchten $1/\alpha$ parameter. The results are presented as look-up tables of seepage rates and their uncertainties, to be used as input to PA. Furthermore, the effects on seepage resulting from excavation-induced drift degradation (i.e., drift collapse) and the presence of rock bolts are also calculated.

This section first discusses the processes and features involved in the SMPA. Then, the geometry used and the ranges of parameters will be described, and the choice of conditions presented and rationalized. Finally, results are given, together with a discussion of alternative models.

Key scientific notebooks (with relevant page numbers) used for modeling activities described in this Model Report are listed in Table 6-1.

Table 6-1. Scientific Notebooks

LBNL Scientific Notebook ID	Citation	M&O Scientific Notebook Register Identification Number	Page Numbers
YMP-LBNL-CFT-GL-2	Wang 2003 [162319]	SN-LBNL-SCI-189-V1	136–151
YMP-LBNL-DSM-MC-1	Cushey 2000 [153481]	SN-LBNL-SCI-052-V1	1–42
YMP-LBNL-SAF-3	Wang 2003 [162319]	SN-LBNL-SCI-228-V1	38–41
YMP-LBNL-JR-2	Wang 2003 [162319]	SN-LBNL-SCI-204-V2	149–163

Note that the results in this Model Report (Rev 02) are very different from those of the earlier version (Rev 01). This is because these new results made use of information from the revised SCM (BSC 2003 [162267], Sections 5 and 6), and the following changes were adopted:

(1) The SMPA uses the same conceptual framework as in the SCM, with the same level of grid-design refinement. Thus, the SMPA is consistent with the SCM, enabling the SMPA to take full advantage of the SCM, which has been calibrated to account for features not explicitly modeled, such as surface roughness of the drift walls.

(2) New calibrated parameters from the SCM (BSC 2003 [162267], Table 16) are used with other information to guide the selection of parameter ranges.

(3) Twenty realizations of the heterogeneous permeability fields are used for each case in the main simulations as a function of mean fracture permeability, inverse van Genuchten α parameter, and percolation flux, thus allowing an estimate of the spread of results from a geostatistical representation of the site. For supplementary sensitivity studies, 10 realizations are used for each case.

6.2 THE SMPA AND THE PHYSICAL PROCESSES

The SMPA builds on the SCM (BSC 2003 [162267], Section 6), and is also described in Birkholzer et al. (1999 [105170], pp. 358–362). The SCM provides the scientific and technical background for this Model Report. The conceptual model is a drift opening in a heterogeneous permeability field representing the fracture continuum, generated with parameters discussed below, using the SISIM module of the GSLIB package (LBNL 2000 [153100]).

Water that penetrates the ground surface and reaches a depth that is unaffected by evapotranspiration, percolates downwards under gravity and capillary forces. The detailed flow paths are determined by the degree of fracturing, fracture geometry, orientation, and connectivity, as well as the hydrogeologic properties of the fractures and the matrix. Depending on these factors, the continuous water phase in the unsaturated fracture network will either disperse or focus along flow paths or channels. Tilted contacts between hydrogeologic units (especially between welded and nonwelded tuffs) may affect the overall flow pattern and lead to a change in the frequency and spacing of flow channels. Flow focusing and dispersion of flow paths also happens *within* a rough-walled fracture, where asperity contacts and locally larger fracture openings lead to small-scale redistribution of water within the fracture. A general discussion of channeling effects under unsaturated flow conditions can be found in Birkholzer and Tsang (1997 [119397]). Flow focusing is important for seepage, because seepage depends on the local percolation flux at the approximate scale of the average fracture spacing.

As water approaches a waste emplacement drift (one to several meters from the drift ceiling), conditions change in several ways, all affecting the amount of water that will eventually seep into the opening. The water may first encounter a dryout zone caused by drift ventilation. The dryout zone may also develop as a result of increased temperature, in which case it is referred to as a boiling zone. Under these thermal conditions, the dryout zone may be surrounded by a two-phase zone in which heat-pipe effects determine water, vapor, heat fluxes, and a condensation zone with increased saturation.

In addition, formation properties around the openings are likely to be altered as a result of stress redistribution during drift excavation. This alteration leads to local opening or partial closing of fractures and potentially the creation of new fractures. Thermal expansion of the rock matrix may also induce changes in apertures. Finally, the local chemical environment, which is altered by evaporation and thermal effects, may lead to dissolution and precipitation of minerals, again affecting porosity, permeability, and capillarity of the fracture system as well as fracture-matrix interaction. All these conditions lead to a flow pattern in the vicinity of a waste emplacement drift different from that in the undisturbed formation under ambient conditions.

Assuming that liquid water penetrates the boiling or dryout zone, it reaches the immediate vicinity of the drift wall, where (at least under ambient conditions) a layer of increased saturation is expected to develop as a result of the capillary barrier effect of the drift opening (Philip 1989 [152651]). The water is prevented from seeping into the drift because of capillary suction, which retains the wetting fluid in the pore space of the rock. This barrier effect leads to a local saturation build-up in the rock next to the interface between the geologic formation and the drift. If the permeability as well as the capillarity of the fracture network within this layer is sufficiently high, all or a portion of the water is diverted around the drift under partially saturated

conditions. Locally, however, the water potential in the formation may be higher than that in the drift, and then water exits the formation and enters the drift.

6.2.1 Features, Events, and Processes Addressed

The features, events, and processes (FEPs) listed in Table 6-2 are addressed in the present Model Report. They are taken from the LA FEP List (DTN: MO0301SEPFEPS1.000 [161496]), with descriptions slightly modified to apply to this Model Report. The LA FEP List is a revision to the previous project FEP list (Freeze et al. 2001 [154365]) used to develop the list of included FEPs in the *Technical Work Plan for: Performance Assessment Unsaturated Zone* (BSC 2002 [160819], Table 2-6). The cross-reference for each FEP to the relevant section (or sections) of this report is also given below. The UZ Departments documentation for the FEPs listed in Table 6-2 is compiled from this and other model reports and can be found in the model abstraction reports as described in Section 2.1.2, Tables 2-3a through 2-3g of the TWP (BSC 2002 [160819]), and the UZ FEPs AMR as described in Section 1.12.10, Table 1.12-1 of the TWP (BSC 2002 [160819]).

Table 6-2. FEPs Addressed in This Model Report

FEP No.	FEP Name	Summary Description
1.1.01.01.0B	Influx through holes drilled in drift wall or crown	Detailed simulations are made of the effect of a rock bolt in drift crown on potential seepage into the drift. See Section 6.5.
1.2.02.01.0A	Fractures	Fracture properties are taken from post-excavation air-permeability data and through calibrated seepage-relevant fracture continuum capillary-strength parameter. See Sections 6.3.2–6.3.4.
1.3.01.00.0A	Climate change, global	The change in percolation flux at the repository level due to climatic change is accounted for by a choice in the range of flux values to cover those changes. See Section 6.3.6
1.4.01.01.0A	Climate modification increases recharge	The change in percolation flux at the repository level due to climatic change is accounted for by a choice in the range of flux values to cover those changes. See Section 6.3.6.
2.1.08.01.0A	Water influx at the repository	An increase in the unsaturated water flux at the repository affects thermal, hydrological, chemical, and mechanical behavior of the system. Increases in flux could result from climate change, and the flux will increase probability of seepage. See Section 6.3.6.
2.1.08.02.0A	Enhanced influx at the repository	The impact of an underground opening on the unsaturated flow field (including dryout from evaporation, capillary barrier effect, and flow diversion around the drift) is captured in the seepage process model by solving the equations governing unsaturated flow in fractured porous media and by specifying appropriate boundary conditions at the drift wall. It leads to reduced (not enhanced) influx. See Section 6.3.6.

Table 6-2. FEPs Addressed in This Model Report (Continued)

FEP No.	FEP Name	Summary Description
2.2.01.01.0A	Mechanical effects of excavation/ construction in the near field	Excavation effects are taken into account through the use of post-excavation air-permeability data and the estimation of a capillary-strength parameter determined from seepage data that reflect seepage from an excavation-disturbed zone around a drift. See Sections 6.3.2 and 6.4.
2.2.03.01.0A	Stratigraphy	Stratigraphic information is necessary information for the performance assessment. For seepage into drift, the Tptpmn and Tptpll units at the repository level are considered. See Sections 6.3.2–6.3.4.
2.2.03.02.0A	Rock properties of host rock and other units	Location-specific rock properties are taken (1) from UZ Model, (2) from local air-permeability data (including measures of heterogeneity and spatial correlation), and (3) from inverse modeling. Variability is accounted for on various scales. See Sections 4.1, 6.3.2–6.3.4.
2.2.07.02.0A	Unsaturated groundwater flow in the geosphere	Unsaturated flow processes are accounted for in the conceptual and mathematical model. See Section 6.2, 2nd and 5th paragraphs, and Section 6.3, 5th paragraph.
2.2.07.03.0A	Capillary rise in the UZ	The effects of capillary forces on flow in the UZ are accounted for in the conceptual and mathematical model. See Sections 6.2 and 6.3.4
2.2.07.04.0A	Focusing of unsaturated flow (fingers, weeps)	Explicitly modeled heterogeneity induces flow focusing. Impact of small-scale flow focusing effects on seepage is included in effective parameters. See Sections 6.3.3 and 6.3.5.
2.2.07.08.0A	Fracture flow in the UZ	Liquid flow through unsaturated fractures is simulated using site-specific fracture properties; explicit inclusion of heterogeneity leads to flow channeling. See Sections 6.3.2–6.3.3
2.2.07.09.0A	Matrix imbibition in the UZ	Matrix imbibition is considered small under steady seepage conditions and is therefore neglected. See Section 6.3, 6th paragraph.
2.2.07.18.0A	Film flow into the repository	Water entering waste emplacement drifts occur by a film flow process. This differs from the traditional view of a flow in a capillary network where the wetting phase exclusively occupies capillaries with apertures smaller than some level defined by the capillary pressure. As a result, a film flow process could allow water to enter a waste emplacement drift at non-zero capillary pressure. Dripping into the drifts could also occur through collection of the film flow on the local minima of surface roughness features along the crown of the drift. For seepage evaluation, this effect is implicitly accounted for through calibration of the SCM against field data. See Section 6.3, 4th paragraph.
2.2.07.20.0A	Flow diversion around repository drifts	The impact of an underground opening on the unsaturated flow field (including capillary barrier effect and flow diversion around the drift) is captured in the seepage process model by solving the equations governing unsaturated flow in fractured porous media and by specifying appropriate boundary conditions at the drift wall. See Section 6.2, 5th paragraph.
2.2.07.21.0A	Drift shadow forms below repository	Drift shadow is simulated as a result of seepage exclusion. See Section 6.6.1.

6.3 THE SMPA AND SELECTION OF PARAMETER RANGES

Similar to the SCM (BSC 2003 [162267]), the continuum approach is used in the SMPA to calculate percolation flux and drift seepage at Yucca Mountain. It is considered appropriate for seepage studies if it is capable of predicting seepage rates for a drift in the fractured formation at Yucca Mountain. Though water flow and seepage from the tuff formation at Yucca Mountain occurs predominantly through the fracture network, it is important to recognize that flow diversion around the drift opening occurs *within* the fracture plane. As flow within the fracture plane encounters the drift opening, which acts as a capillary barrier, it is diverted around it, as described by Philip et al. (1989 [105743]). This process is appropriately captured by a two-dimensional (2-D), heterogeneous fracture continuum model even for a single fracture. In-plane flow from multiple fractures can be readily combined into a 3-D fracture continuum. The need to engage multiple fractures arises only if the flow path within the fracture plane is insufficient for flow diversion around the drift.

At Yucca Mountain, the formation at the repository horizon has a high fracture density, and these fractures form a well-connected 3-D system at all scales. This is evidenced in fracture data from the Exploratory Studies Facility (ESF) main drift. An examination of the data (Cushey 2000 [153481], pp. 40–42) shows the presence of many fractures, from very short to 3 m or more, and that the fracture spacings are less than fracture trace lengths for each cumulative subset of fractures (see also BSC 2001 [156304], Table 6). Further, Table 5 of BSC (2001 [156304]) indicates that the fracture sets in Tptpmn and Tptpll (lower lithophysal zone of the Topopah Spring Tuff) units span 3-D orthogonal directions. These data together indicate a well-connected, densely fractured medium that can be represented by a fracture continuum. Thus, a 3-D, heterogeneous fracture-continuum model captures the relevant processes more realistically than, for example, a 2-D discrete-fracture-network model.

In addition, the appropriateness of the continuum approach to simulate flow through fractured rock was studied by Jackson et al. (2000 [141523]), using synthetic and actual field data. They concluded that heterogeneous continuum representations of fractured media are self-consistent, i.e., appropriately estimated effective continuum parameters are able to represent the underlying fracture-network characteristics.

Furthermore, Finsterle (2000 [151875]) demonstrated that simulating seepage into underground openings excavated from a fractured formation could be performed using a continuum model, provided that the model is calibrated against seepage-relevant data (such as data from liquid-release tests). Synthetically generated data from a model that exhibits discrete flow and seepage behavior were used to calibrate a simplified fracture continuum model. The calibrated continuum model was used to predict average seepage rates into a sufficiently large section of an underground opening under low percolation flux conditions. Thus, the study corresponds to the extrapolation from the calibration runs against high-rate liquid-release tests performed with the SCM to the predictive simulations that are performed by the SMPA. As discussed in Finsterle (2000 [151875]), the extrapolated seepage predictions performed with the continuum model were consistent with the synthetically generated data from the discrete fracture model under low percolation conditions. This demonstrates that (1) the calibrated continuum model and discrete fracture model yield consistent estimates of average seepage rates, and (2) that the continuum approach is appropriate for performing seepage predictions even if extrapolated to percolation

fluxes that are significantly lower than the injection rates of the liquid-release tests used for model calibration.

Within the continuum approach, relative permeability and capillary pressure are described as continuous functions of effective liquid saturation, following the expressions given by the van Genuchten-Mualem model (van Genuchten 1980 [100610], pp. 892–893) as implemented in the iTOUGH2 code (BSC 2002 [161066], Section 4.3.2). Capillary strength (represented by the $1/\alpha$ parameter) and permeability are not correlated, because the functional relationship describing the potential correlation between permeability and capillary strength is unknown for a fractured medium. An increase in permeability may be attributed to larger fracture apertures (which would reduce capillary strength) or to an increase in fracture density (which would not affect capillary strength). The capillary-strength parameter $1/\alpha$ is taken to be constant for a given test bed, and its value is to be estimated through calibration. In this, the SMPA has the same formulation as the SCM, and the consistent conceptualization in the SMPA and the SCM make this a valid approach. The SMPA provides results on seepage for a wide range of permeability and capillary-strength values. However, the use of the results should center on the SCM calibrated values and explore variations from them. This will avoid a combination of extreme choices of these two parameters that may represent a nonphysical condition.

Within the SMPA, the flux exchange between fractures and matrix in a steady-state fracture-matrix system is negligible and does not need to be modeled explicitly in the SMPA. In general, matrix permeability is low, and the potential for imbibition of substantial amounts of water into the matrix is limited, because of its relatively low porosity and relatively high initial liquid saturation. In a fracture-matrix system, the transient flow between fracture and matrix is restricted to intermediate times, i.e., they are insignificant (1) for a short-term liquid-release test with insufficient time for matrix imbibition and (2) for a long-term seepage experiment, in which near-steady late-time data are no longer affected by matrix imbibition. The ability of a single fracture-continuum model to reproduce and predict average seepage from a discrete fracture-matrix system has been demonstrated by Finsterle (2000 [151875]) using synthetic data.

Also within the SMPA, the effect of lithophysal cavities on seepage is represented through the use of an effective capillary-strength parameter, without the explicit inclusion of lithophysal cavities into the process model. This approach is considered appropriate for the following reasons: (1) the effect of lithophysal cavities is included by the SCM (BSC 2003 [162267]) in the calibration conditioned to data from Tptpll testing; (2) because of capillary effects, flow will be mainly through fractures rather than the cavities; and (3) omitting lithophysal cavities is consistent with the SCM, and consistency between the calibration model (the SCM) and the prediction model (the SMPA) removes the impact of a potential bias.

6.3.1 Drift Geometry and Grid Design

As provided in design drawings 800-IED-EBS0-00200-000-00A (BSC 2002 [160798]) and 800-IED-EBS0-00100-000-00A (BSC 2002 [160317]) respectively, the drift diameter is 5.5 m and the waste package length is 5.1 m. The 3-D calculational domain for this Model Report is chosen to be 10 m high, 4 m wide, and 2.4384 m long, covering the upper left-hand half of the drift with diameter of 5.5 m (See Figure 6-1). Thus a vertical plane through the axis of the drift forms the right-hand boundary, and the drift axis is 0.5 m above the lower boundary. The length along the

drift axis is chosen to be 8 ft (2.4384 m), which is 8 grid cells of 1 foot (0.3048 m) length. Thus, the calculated seepage will be over an area of half the drift (cut along its axis) and the length of 2.4384 m, which amounts to an area of (5.5/2) × 2.4384 = 6.706 m^2. On the other hand, the cross-sectional area of the drift containing one waste package is 5.1 × 5.5 = 28.05 m^2. Consequently, the seepage rate at steady state calculated in the simulation domain needs to be scaled-up by a factor of (28.05/6.706 = 4.183) to obtain the seepage rate for the full drift per waste package, expressed as m^3 of water per year per waste package (m^3/yr/wp). Seepage percentage is defined as this seepage rate divided by the product of percolation flux (m/yr), the diameter of the drift (5.5 m), and the length of the waste package (5.1 m). This product is the amount of percolation water incident on the footprint of the drift section with one waste package. The calculation of seepage percentage does not require consideration of the scale-up factor of 4.183, if the calculated seepage from this model is divided by the total percolation water incident on the model area of 6.706 m^2.

The grid cells in the plane normal to the drift axis are 0.1 × 0.1 m. The limited size of the calculational domain was chosen to allow the use of a fine mesh at the same refinement level as the SCM, and yet contain a reasonable number of grid cells so as not to make the computational time too long. The left-hand boundary is placed at (4–2.75) = 1.25 m beyond the left-hand limit of the drift to capture the main flow feature, i.e., flow diversion around the drift (Philip et al. 1989 [105743], p. 21, Figure 1). The side boundary conditions are no-flow, and the lower boundary condition is gravity drainage, implemented by setting the capillary pressure gradient to zero across the bottom connections. The upper boundary surface is simulated by an extra grid cell with constant percolation flux connected to all the grid cells in the first row. Flow is thus free to move into these cells according to local property parameters. Since all calculations were run to steady state, the initial conditions are not important and are set to zero saturation over the domain.

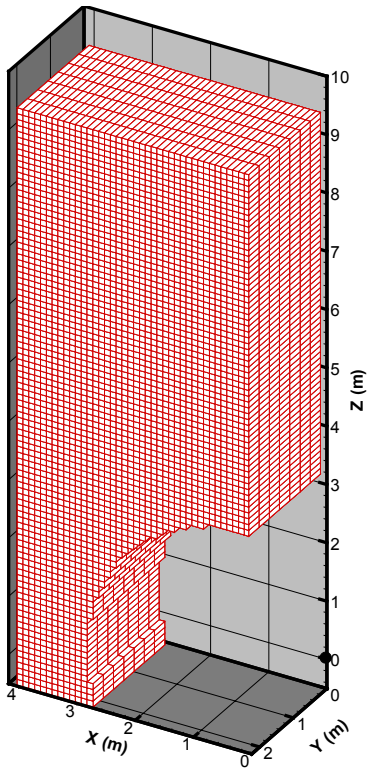

Output - DTN: LB0304SMDCREV2.002

NOTE: As shown, the lines are drawn through the centers of grid cells and not the sides, so that *n* lines shown represent *n* cells and not (*n*-1) cells.

Figure 6-1. Model Domain and Mesh Design. The point shown at (z = 0 and x = 0) indicates the axis of the drift.

Regarding the no-flow boundary condition on the two planes normal to the drift axis and on the right-hand vertical boundary: for a homogeneous, constant-property medium, these planes are symmetry planes, and a no-flow boundary condition is justified. For a heterogeneous system, the issue is the length of the flow domain versus the spatial correlation length λ. Except for the cases used in a sensitivity study of the spatial correlation length, the spatial correlation length λ is chosen to be 0.3 m (see Section 6.3.5 below). Thus, the length of flow domain in the direction of the drift axis is 8 times the spatial correlation length, and its width is 13 times the correlation length. Given this setup, no-flow boundaries should not have a significant effect on flow results.

At the drift wall, the nodal distance between the drift surface and the grid cell representing the drift is set to be very small, so that the boundary condition can be applied directly at the drift wall. The length of the last vertical connection between the drift wall and the neighboring gridblocks representing the formation is set equal to 0.05 m, to make this model consistent with the SCM (BSC 2003 [162267]). The choice of this 0.05 m vertical connection to the drift wall implies a direct gravity-controlled vertical flow, with no horizontal diversion, over this 0.05 m distance.

Flow calculation was performed using iTOUGH2 V5.0 (LBNL 2002 [160106]). The selection of parameter ranges and particular cases to be modeled is based on available relevant data and is presented below, along with the rationale for the selection. Much information and data are available for the Topopah Spring middle nonlithophysal zone (UZ model layer tsw34, lithostratigraphic unit Tptpmn). However, additional data from the lower lithophysal unit have also been analyzed in the SCM (BSC 2003 [162267]); the parameter values for this unit are also covered by the selected range of parameters. The parameters most likely to affect drift seepage are fracture continuum permeability k_{FC}, van Genuchten $1/\alpha$ value, and the percolation flux Q_p. For each combination of these three parameters (i.e., at each grid point in 3-D parameter space), seepage model calculations will be made for 20 realizations of the generated heterogeneous permeability field.

Though the choices of parameter ranges for which seepage calculations are performed are based on a review of available relevant data, these data are not directly used as input to the model to produce seepage results, but rather as references to establish parameter ranges.

6.3.2 Fracture Continuum Permeability k_{FC}

For the SMPA, a range of k_{FC} values needs to be established, that, when coupled with other parameters, forms a set of cases. Potential seepage rates as a function of percolation flux on top of the simulation domain are then calculated for each case. The k_{FC} range has been selected based on a review of the available site data at Yucca Mountain (see below) and the needs of the upcoming revision of the Seepage Abstraction Model (CRWMS M&O 2001 [154291]). The series of k_{FC} values in terms of $\log_{10} k_{FC}$ (m^2) are from –14 to –10, at steps of 0.25. Data and information leading to the selection of this group of k_{FC} values are described below.

A number of air-permeability measurements have been made in the Topopah Spring middle nonlithophysal unit. BSC (2003 [161773]) presents a systematic study of these data, and Table 7 of BSC (2003 [161773]) indicates that the mean $\log_{10} k_{FC}$ values for Tptpmn (tsw34) unit are about –12.81 to –12.48, values without the effect of excavation. For drift seepage simulations, what is probably more suitable are the post-excavation data, which accounted for stress release due to the excavation, resulting in a change in fracture permeabilities in the rock near the drift wall. BSC (2003 [162267], Table 10) presents an analysis of post-excavation data and gives the mean $\log_{10} k_{FC}$ for Tptpmn unit as –12.14 to –11.66 (Niches 3107, 3650, and 4788 in the Table) $\log_{10}$ with a mean of –11.86. Thus, there is an increase of about 1.2 to 0.3 in $\log_{10}$ compared with the pre-excavation values. BSC (2003 [163501]) conducted a coupled thermal-hydrological-mechanical analysis of rock permeability changes on the drift scale. This analysis shows (BSC 2003 [163501], Figure 6.4.1-1) that drift excavation induces a change in vertical permeability, averaged over 1 drift radius above the crown of the drift, of about 1.3 ($\log_{10}$ change of 0.11) and a change in horizontal permeability, in the same region, of about 10 ($\log_{10}$ change of 1.0). For drift seepage, a larger increase in horizontal permeability and a small increase in vertical permeability near the drift crown will facilitate the flow of water laterally around the drift and hence reduce seepage probability. Also, note that the flow diversion effect of the capillary barrier, as presented by the drift, acts in a rock layer very close to the drift wall. The thickness of this rock layer depends on the capillary strength. For a van Genuchten $1/\alpha$ parameter of 600 Pa, this thickness is less than 20 cm. BSC (2003 [163501]) shows a horizontal permeability increase of 10 or more extending about 0.5 m into the rock above the crown of the drift. Further

discussions on excavation enhanced k_{FC} values are given in Section 6.7 and also in BSC (2003 [163501]).

For the Tptpll unit, there are much less data. They are found from measurements in Niche 1620 and the borehole SYBT-ECRB-LA#2. Generally the air permeability values are an order of magnitude larger than those of the Tptpmn unit. BSC (2003 [162267], Table 10) presents an analysis of the data and gives the mean $\log_{10} k_{FC}$ (m^2) from Niche 1620 data as –10.95 and that from SYBT-ECRB-LA#2 as –10.73, with an average of –10.84. These numbers are within the range chosen for the $\log_{10} k_{FC}$ parameter, –14 to –10.

6.3.3 Standard Deviation of log k_{FC}

For the three niches (Niches 3107, 3650, and 4788) in the middle nonlithophysal zone, the SCM (BSC 2003 [162267], Table 10) gives values for the standard deviation σ of fracture continuum permeability in log base 10, which vary from 0.72 to 0.84. For the lower lithophysal unit, the same source gives a log base 10 standard deviation of 0.21 for the ECRB test and 1.31 for the niche test.

In a numerical study of seepage from a heterogeneous fracture continuum into a drift, Birkholzer et al. (1999 [105170], p. 371, Figure 14) found that drift seepage tracks the probability for finding local ponding in the heterogeneous field and, further, that the ponding probability is smaller for smaller permeability standard deviations (Birkholzer et al. 1999 [105170], p. 375, Figure 17). Hence, less seepage is expected for smaller σ values. This Model Report uses $\sigma = 1.0$ as the base case. Then a sensitive study on seepage rates will be made for $\sigma = 0.5$ and 2.0, and the results compared with those of $\sigma = 1$. It is shown (Section 6.6.2) that while the calculated seepage percentage is sensitive to σ for low σ values, it does not vary much for $\sigma = 1$ to 2.

6.3.4 van Genuchten Parameters

It is a conclusion from the SCM analysis (BSC 2003 [162267], Section 6.6.3.1) that seepage is not sensitive to the van Genuchten parameter *n*. Therefore, in this analysis, *n* is not varied, but set to 2.55 (corresponding to the van Genuchten parameter $m = (n–1)/n = 0.608$, Table 4-2). This is consistent with the approach in the SCM (BSC 2003 [162267]). This value of m is used for both the Tptpmn and Tptpll units. Table 4-2 gives m values for the Tptpll unit to be 0.611; the 0.5% change of this parameter will have negligible impact on simulation results of this Model Report.

In the SCM (BSC 2003 [162267], Table 16), the $1/\alpha$ values have a calibrated mean of 582 Pa in the lower lithophysal unit, with standard deviation of 105 Pa. For the middle nonlithophysal zone, the SCM (BSC 2003 [162267], Table 16) gives the calibrated mean for $(1/\alpha)$ as 604 Pa, with the standard deviation of 131 Pa. In this Model Report, ten $1/\alpha$ values, namely 100 to 1000 Pa, at 100 Pa steps, are chosen to cover well beyond these numbers.

6.3.5 Spatial Correlation Length λ of k_{FC}

In general, this is a difficult parameter to determine in the field. As indicated by the SCM (BSC 2003 [162267], Section 6.6.2.1), the analysis of air-injection tests suggests that “the permeability

is random without a noticeable or significant spatial correlation" for the middle nonlithophysal zone. These results can be taken to indicate a spatially uncorrelated structure. Thus, for the main set of calculations covered in this report, the spatial correlation length is set equal to grid size in the direction of the drift axis, i.e., 0.3 m, and apply this also to the plane normal of the drift axis. Since grid size in the normal plane is 0.1 m, this correlation length is equal to 3 grid lengths in this plane.

Since λ is not an easily determined parameter *in situ*, cases with alternative λ values were calculated to investigate its sensitivity. Cases with $\lambda = 1$ m and $\lambda = 2$ m are calculated, and ten realizations of the heterogeneous field are considered for each of these cases.

6.3.6 Percolation Flux, Q_p

For the SMPA calculations, 15 values of Q_p are used, ranging from 1 to 1,000 mm/yr; or, more specifically, $Q_p = 1$, 5, 10, 20, 50, and then 100 to 1000 mm/yr at 100 mm/yr steps. The range is chosen to cover various estimates of percolation fluxes. Wu et al. (1999 [117161], p. 210) calculated the percolation flux expected at the repository level, based on a 3-D UZ model of Yucca Mountain. They obtained an average fracture flow of 4 to 5 mm/yr at the repository level under present climate conditions. Ritcey and Wu (1999 [139174], p. 262) found that under a climate scenario simulating the most recent glacial period, the percolation flux at the repository level ranges from 0 to 120 mm/yr, with the peak of the probability distribution to be around 20 mm/yr. More recent predictions of percolation flux have been summarized in DTN: LB0302PTNTSW9I.001 [162277]. These are reviewed to arrive at the parameter range used in this Model Report. In particular, the upper limit of Q_p is chosen to accommodate potential flow focusing in the geologic layers above the drift and to safely bracket a large uncertainty range.

6.3.7 Summary on Parameter Ranges

Table 6-3 shows parameter values for simulations in two categories. The first category is an extensive set of systematic calculations conducted for all combinations of $\log_{10} k_{FC}$ (m^2), $1/\alpha$ (Pa) and Q_p (mm/yrs) values shown in the table. Standard deviations of seepage rates over 20 realizations of the heterogeneous permeability field are also evaluated. Second, sensitivity studies are made for σ of $\log_{10} k_{FC}$ and λ, with 10 realizations for each case.

Table 6-3. Ranges of Key Parameters

Parameter	Values
Systematic Simulations (20 Realizations)	
$\log_{10} k_{FC}$ (m^2) $1/\alpha$ (Pa) Q_p (mm/yr)	–14.0 to –10.0 (steps of 0.25) 100 to 1000 (steps of 100) 1, 5,10, 20, 50, 100 to 1000 (steps of 100)
Sensitivity Studies: log10 k_{FC} (m2) = –12; $1/\alpha$ = 600 Pa; Q_p = 200 mm/yr (10 realizations)	
σ of $\log_{10} k_{FC}$ (m^2)	0.5, 1.0 (Base Case), 2.0
λ (m)	0.3 (Base Case), 1.0, 2.0

Output - DTN: LB0304SMDCREV2.001

6.4 IMPACT OF DRIFT DEGRADATION ON SEEPAGE

Because of excavation, stress is redistributed and fractures are generally expected to dilate near the crown of the drift. Such fracture dilation depends on the orientation of the fracture set and generally occurs within one drift radius (Brekke et al. 1999 [119404], Figures E-5, E-11 and E-13). An increase in fracture aperture generally causes an increase in fracture permeability and a decrease in $1/\alpha$ value. The measured increase in permeability from the pre-excavation to the post-excavation values (Wang et al. 1999 [106146], p. 328; DTN: LB0011AIRKTEST.001 [153155]) is a result of this effect. Calibrated parameters from calculations based on *in situ* post-excavation data, as presented by the SCM (BSC 2003 [162267]), have already taken this into account. This means that the rock properties already represent the total effect of the near-field disturbed zone and the far field, and no additional calculations are necessary.

The possibility exists that new fractures may be formed due to the excavation or subcritical crack growth over time. In general, an increase in k_{FC} could result from either an increase in the number of fractures or an increase in apertures. It is only in the latter case that $1/\alpha$ will decrease. The part of increase in k_{FC} resulting from the creation of new fractures will be accompanied by no decrease in $1/\alpha$ values. This scenario is, however, not studied because it would lead to less seepage.

Over time, extended rock failure may also occur at the roof of the drift. Kaiser (Brekke et al. 1999 [119404], pp. D-11, D-12) estimated the failure at the roof to be 0.1–1 m in depth, and 0.4–1.2 m in depth if seismic effects were included. Generally, Kaiser expected stress-induced failure at the drift crown to occur over a distance of 1/2 drift radius, i.e., ~1.375 m. On the other hand, a much more extended failure region up to one drift radius above the drift roof can be assumed (see Section 5). In this Model Report, the authors make a study of the impact of drift degradation using the worst case and 75 percentile cases of degraded drift profiles for Tptpmn and Tptpll units referenced in Section 5. The drift profiles and the fall-off rock volumes are used to construct 3-D cases. This was done first by taking away rock grid cells in a plane normal to drift axis to approximately match the profile in that plane, and then by taking away grid cells along the drift axis to approximately match the fall-off rock volume. Note that since the calculational domain represents only part of the drift (Section 6.3.1 and Figure 6.1), if the rock-fall is across the model boundary, the rock-fall volume is factored accordingly. Now, on these discretized drift profiles, seepage was calculated with 10 realizations of the heterogeneous

permeability field. Calculations were carried out for both the Tptpmn and the Tptpll units. For Tptpmn, available data at three niche locations for $\log_{10}k_{FC}$ are –12.14, –11.66, –11.79 (BSC 2003 [162267], Table 10), with an average of –11.86, which was taken for this particular set of calculations. Similarly for Tptpll, available data for two niche locations are –10.95 and –10.73 (BSC 2003 [162267], Table 10), with an average of –10.84, taken for calculations of seepage into the degraded drifts. The other key parameter values are $1/\alpha$= 600 Pa and Q_p =200 mm/yr. No-degradation results with the same parameter values were also calculated for comparison to study the impact of drift degradation on seepage.

6.5 EFFECTS OF ROCK BOLTS ON SEEPAGE

Using grouted rock bolts is one proposed method of ground support for emplacement drifts at Yucca Mountain (BSC 2001 [155187]). Rock bolts are steel rods grouted into a borehole normal to the drift wall. Typically they are 3 m long (BSC 2001 [155187], Section 6.5.1.2.2) with a diameter of 1 inch (0.0254 m) and a grout annulus thickness of 1/4 inch (0.00635 m) (BSC 2001 [155187], Table 4-10). Rock bolts pose a concern with respect to seepage because they provide a direct flow conduit to the drift wall and may increase the likelihood of seepage into drifts.

A refined model has been prepared that includes a range of properties for the formation and the grout (including “no-grout” for a mechanically anchored bolt), as well as a range of percolation rates. Figure 6-2 shows a sketch of the model. The model uses a two-dimensional, radially symmetric grid with a vertical symmetry axis generated using the software TOUGH2 V1.4 (LBNL 2000 [146496]). Grid size is 10 cm, with finer discretization (down to 0.1 mm) at the interface between the grout and the surrounding rock. Because this is a radially symmetric grid, the drift opening, created using the routines MoveMesh V1.0 (LBNL 2000 [152824]) and CutNiche V1.3 (LBNL 2000 [152828]), is spherical instead of cylindrical. Knight et al. (1989 [154293], p. 37) find that seepage exclusion from a cylindrical cavity is similar to that of a spherical cavity of twice the radius. This is explained by relating the seepage exclusion potential of an opening to the total curvature of the boundary of the opening. For a cylindrical cavity, the radius of curvature is infinite along the axis of the cylinder and finite perpendicular to the axis. For a spherical cavity, the radius of curvature is finite and equal in any direction. As a result, to have the same curvature, the equivalent radius of the spherical “drift” in the model is twice that of the design drift radius. This relationship is used in the calculation of seepage enhancement owing to the presence of rock bolts.

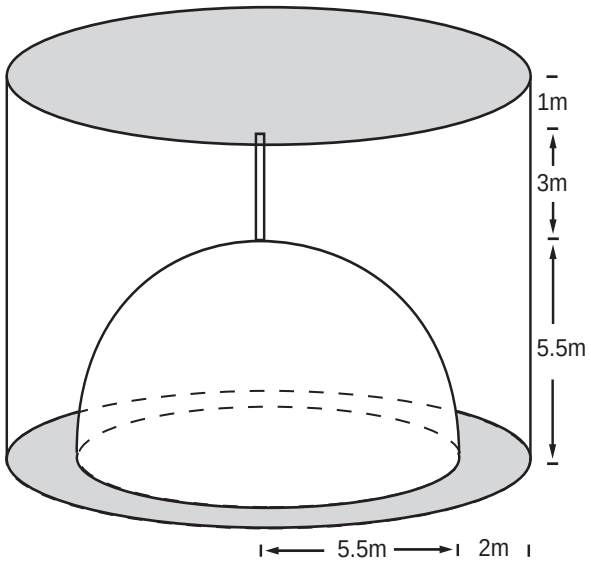

Figure 6-2. Model to Evaluate Impact of Rock Bolt. Note that the radius of the spherical drift is taken to be 5.5 m, making its curvature equal to that of a cylindrical drift with a radius of 2.75 m. The rock bolt hole is at the crown of the drift with length of 3 m.

As a base case, seepage into the opening without any rock bolts is modeled. Since this is treated as a sensitivity study, the low and high percolation rates of 5 and 500 mm/yr are applied uniformly to the upper model boundary. A constant zero capillary pressure is specified at the drift wall boundary, a gravity-drainage condition at the lower boundary (assigned in the grid using the routine AddBound V1.0 (LBNL 2000 [152823])), and a no-flow condition on the lateral boundary. The fracture-continuum permeability is chosen to be the mean of data for the Tptpmn unit, i.e., log K_{FC} = –11.86 (see Section 6.4). The mean value for the Tptpll unit is –10.84 (see Section 6.4), which would allow for more water diversion and less seepage, and hence, it is not calculated. The $1/\alpha$ values of 200 and 400 Pa are used for the rock. An additional calculation with $1/\alpha$ = 589 Pa (a number in between the calibrated values for Tptpmn and Tptpll units, BSC 2003 [162267], Table 16) was also made, as part of the sensitivity analysis.

To investigate the impact of a rock bolt on seepage, only the case of a rock-bolt borehole extending vertically upward from the crown of the drift is modeled. If there is negligible effect, then this case is sufficient to resolve the question of impact on seepage caused by the presence of the rock-bolt borehole. Three slightly different grids are prepared to explore diversion capacity away from the rock-bolt borehole. Case 1 allows flow between the rock-bolt borehole and the surrounding rock along the entire length of the rock-bolt hole. Case 2 prevents flow between the rock-bolt borehole and the surrounding rock for 10 cm above the crown of the drift. Case 3 restricts flow between the rock-bolt borehole and the surrounding rock for 50 cm above the crown of the drift. Cases 2 and 3 represent scenarios in which the first feature capable of carrying flow away from the rock-bolt borehole is found 10 cm or 50 cm, respectively, into the borehole. A 1-inch (0.0254 m) radius rock-bolt borehole with a ½-inch (0.0127 m) radius rock bolt and a ½-inch (0.0127 m) grout annular thickness is modeled. The modeled grout annular thickness is twice as large as the design value (BSC 2001 [155187], Table 4-10). This configuration results in a conservative model, because the modeled bolt hole has less potential as a capillary barrier to exclude in-flow, but a larger surface area to intercept flow, thus allowing a greater opportunity to conduct flow to the drift wall.

Because the greatest impact of the rock bolts on seepage may come many thousands of years in the future (after cool down and rewetting of the repository horizon), the grout is not likely to retain its designed hydraulic properties. It may even completely disintegrate, leaving an open hole. So, for the present sensitivity studies, instead of single values, a range of properties for the grout is used. Figure 6-3 shows the combinations of grout properties evaluated. In particular, shown in the lower left is a combination (case G1), where the grout permeability equals 10^{-18} m^2 and $1/\alpha$ equals 10^7 Pa, corresponding to a slightly degraded grout. The upper right shows a combination (case G2) in which the grout permeability equals 10^{-10} m^2 and $1/\alpha$ equals 10 Pa, which corresponds essentially to an open rock-bolt borehole. Thus, the G2 case particularly corresponds to the case of an open, mechanically anchored bolt design.

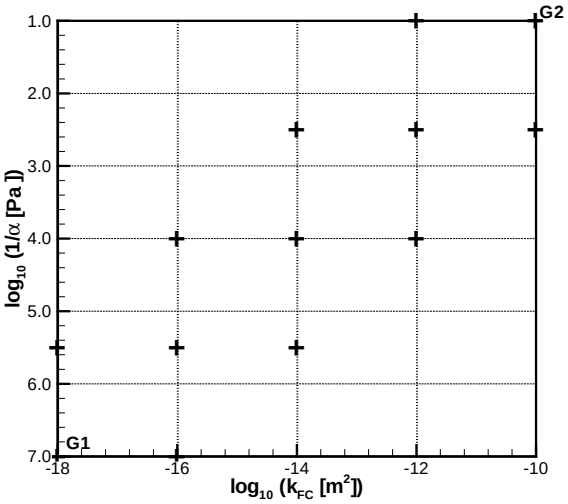

Output - DTN: LB0304SMDCREV2.002

Figure 6-3. Grout Parameter Combinations

6.6 RESULTS

Seepage percentage is defined as the ratio of the seepage rate into a drift section to the percolation rate applied to the top of the model over the projected cross-sectional area of that drift section.

6.6.1 Seepage over (k_{FC}, $1/\alpha$, Q_p) Space

Figure 6-4a gives the calculated seepage rate in cubic meters of water per year per waste package (m^3/yr/wp) as contour sheets in a space spanned by $\log_{10}k_{FC,}$ $1/\alpha$, and $Q_{p.}$ This corresponds to simulated total seepage rates into a drift of 5.5 m diameter and 5.1 m length (length of a waste canister). The contour sheets are labeled by the seepage rates averaged over 20 realizations of the generated heterogeneous permeability field. Thus, to get the seepage rate for a particular set of $\log_{10}k_{FC}$, $1/\alpha$ and Q_p values, the corresponding point in 3-D space is located and interpolated between sheets of seepage rate values. In practice, detailed seepage results for all 20 realizations are provided for every combination of k_{FC}, $1/\alpha$, and Q_p values in the form of look-up tables, and are submitted to TDMS (Output-DTN: LB0304SMDCREV2.002). As one would expect, seepage is large for large Q_p, small $1/\alpha$, and small k_{FC} values. The threshold for seepage is shown

as the lowest sheet (red) in the figure. The parameter space below this sheet represents cases in which no seepage is expected to occur.

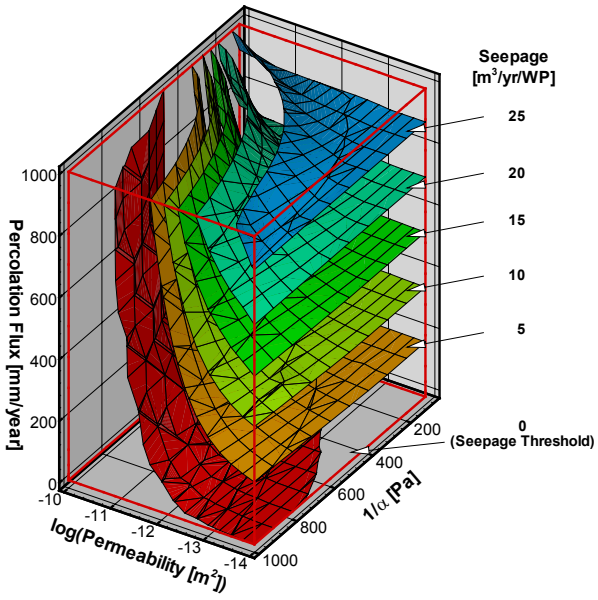

(a)

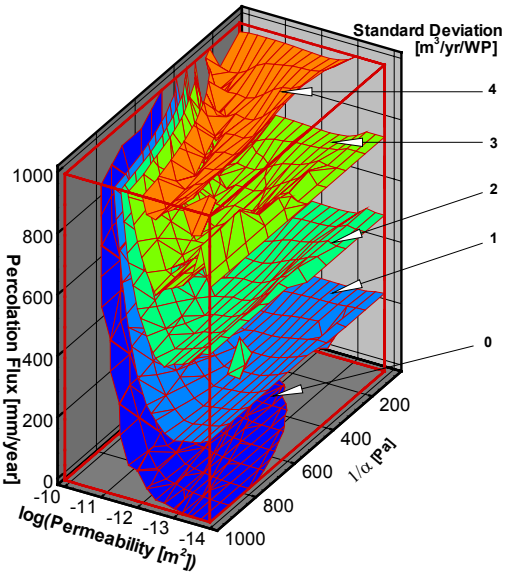

(b)

Output - DTN: LB0304SMDCREV2.002

Figure 6-4. Distribution of Mean (a) and Standard Deviation (b) of Seepage Rate as a Function of Permeability, van Genuchten 1/α, and Percolation Flux

Figure 6-4b shows the standard deviation over the 20 seepage results for the 20 realizations. The arrangement is the same as in Figure 6-4a. Thus, for any particular set of $\log_{10}k_{FC}$, $1/\alpha$, and Q_p parameter values, one can go to Figure 6-4a to obtain the mean seepage rate and then go to Figure 6-4b to obtain the corresponding standard deviation over 20 realizations for this particular case. The results indicate that the geostatistical spread is larger for large seepage rates, and it is generally less than ~20%.

Figure 6-5 corresponds to Figure 6-4a, but expresses the results as seepage percentage. Figures 6-6 to 6-8 show the same results as Figure 6-5, but as mean seepage-percentage contours on planes representing two out of the three parameters. Thus, the calculated results from Figure 6-5 are projected on planes corresponding to constant values for one of the three parameters.

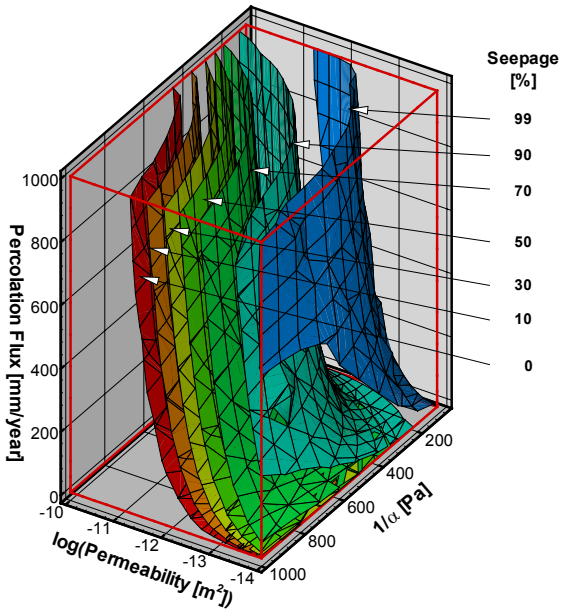

Output - DTN: LB0304SMDCREV2.002

Figure 6-5. Trend of the Mean of Seepage Percentage as a Function of Permeability, van Genuchten 1/α, and Percolation Flux

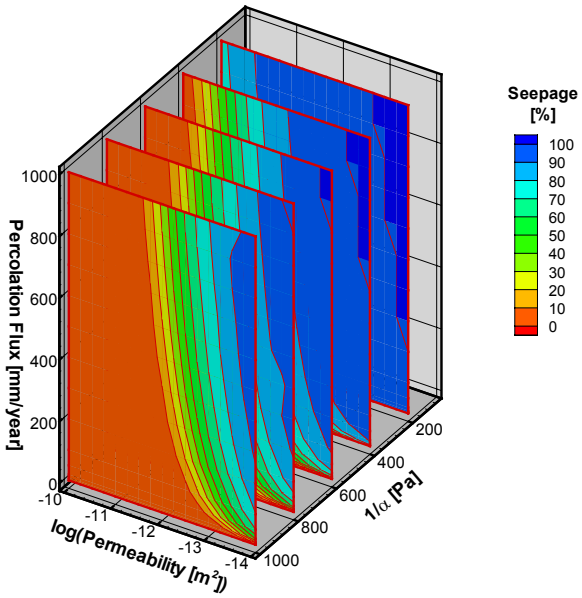

Output - DTN: LB0304SMDCREV2.002

Figure 6-6. The Mean of Seepage Percentage on Vertical Planes of van Genuchten 1/α = 200, 400, 600, 800, and 1,000 Pa Respectively

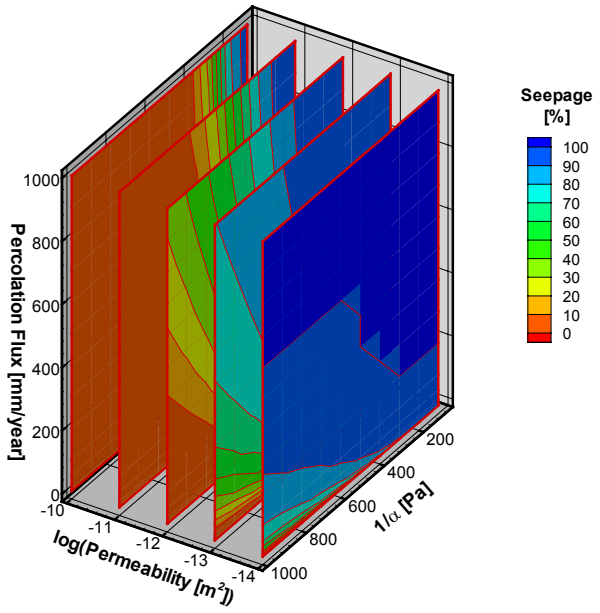

Output - DTN: LB0304SMDCREV2.002

Figure 6-7. The Mean of Seepage Percentage on Vertical Planes of Permeability Field for $\log_{10}k_{FC}$ (m^3) = –14, –13, –12, –11, and –10

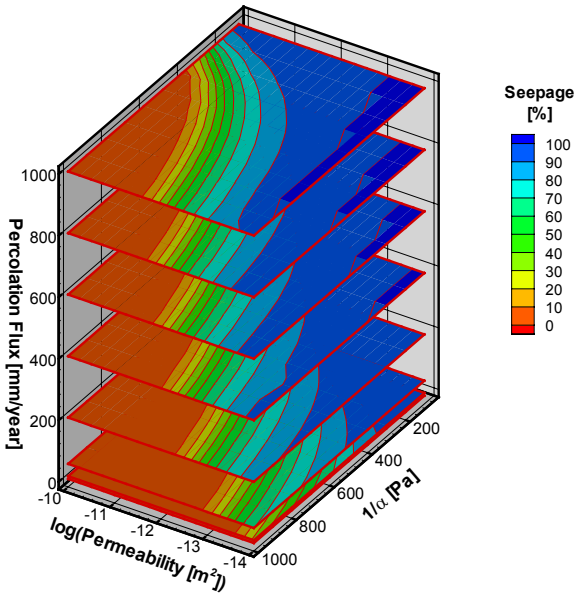

Output - DTN: LB0304SMDCREV2.002

Figure 6-8. The Mean of Seepage Percentage on Horizontal Planes of Percolation Flux for Q_p = 1,10, 50, 200, 400, 600, 800, and 1,000 mm/yr

As a further illustration, dependence of seepage percentage on one of the three parameters (k_{FC}, $1/\alpha$, Q_p), one at a time, is shown in Figures 6-9 to 6-11. In these figures, the red squares show results for each of the 20 realizations, and the blue-filled dots give their average values. These figures demonstrate clearly that seepage decreases with larger k_{FC} and $1/\alpha$, and increases with larger Q_p. They also show that the geostatistical spread is quite large.

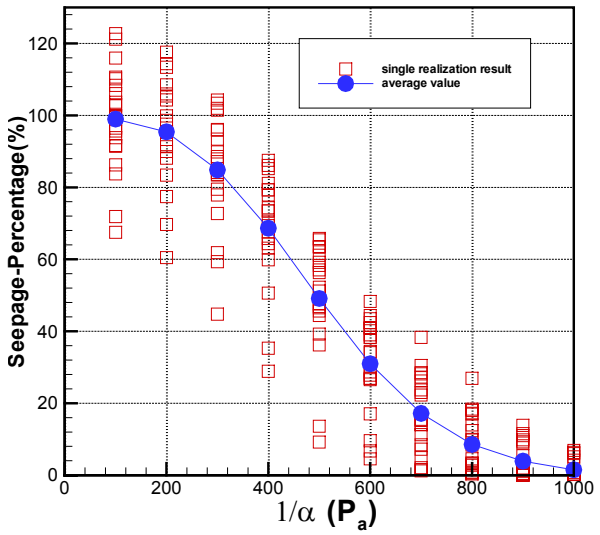

Output - DTN: LB0304SMDCREV2.002

Figure 6-9. Seepage Percentage as a Function of van Genuchten $1/\alpha$, with $\log_{10} k_{FC} = -12$, $Q_p = 200$ mm/yr

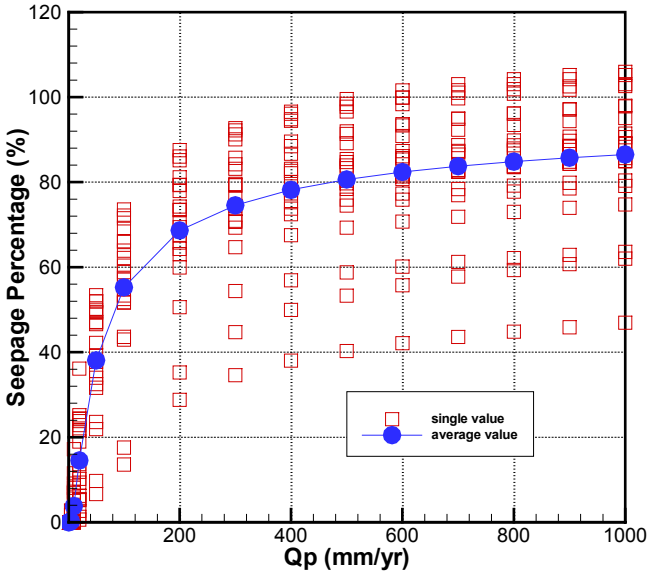

Output - DTN: LB0304SMDCREV2.002

Figure 6-10. Seepage Percentage as a Function of Percolation Flux, with $\log_{10} k_{FC} = -12$, $1/\alpha = 400$ Pa

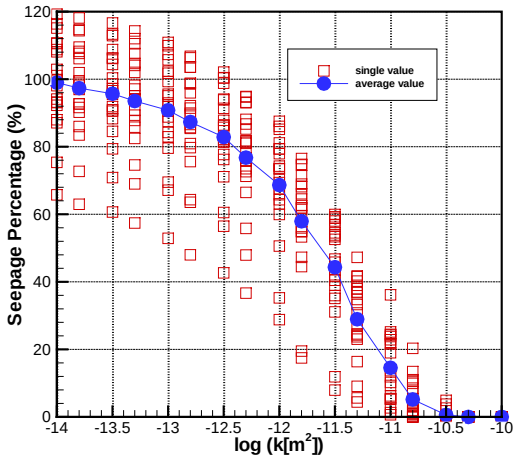

Output - DTN: LB0304SMDCREV2.002

Figure 6-11. Seepage Percentage as a Function of Mean Permeability, with Q_p = 200 mm/yr, $1/\alpha$ = 400 Pa

6.6.2 Sensitivity to λ and σ

The sensitivities of calculated seepage rates to λ and σ values are calculated for one particular combination of parameters, namely:

$\log_{10} k_{FC} = -12.0$
$1/\alpha = 600$ Pa
$Q_p = 200$ mm/yr

This parameter set is chosen to be approximately at the center of the ($\log_{10}k_{FC}$, $1/\alpha$) plane, having a large, but not extremely large, percolation flux rate of 200 mm/yr. In this analysis, 10 realizations of the heterogeneous permeability fields are used.

Figure 6-12 shows the results for three values of λ:

λ = 0.3 m (base case).
λ = 1 m
λ = 2 m

The red squares give results for individual realizations, and the blue-filled circles give the average over the 10 realizations for each case. As can be expected, the geostatistical spread results from the multiple realizations increases with λ.

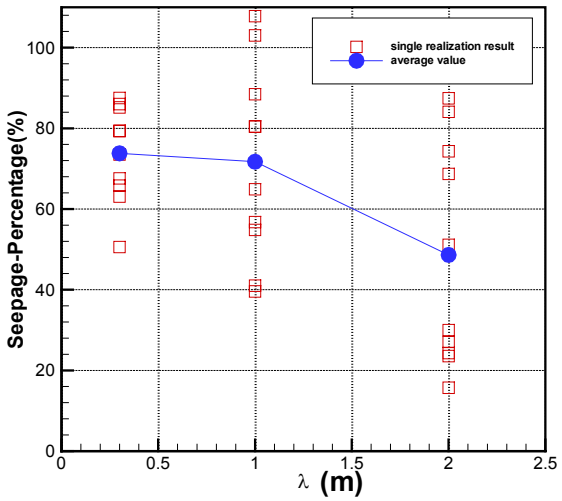

Output - DTN: LB0304SMDCREV2.002

Figure 6-12. Seepage Percentage as a Function of Correlation Length, with $\log_{10} k_{FC} = -12$, $Q_p = 200$ mm/yr, $1/\alpha = 600$ Pa

Figure 6-13 presents the results of sensitivity to the standard deviation, σ, in $\log k_{FC}$ of the heterogeneous permeability field, using the same notation as before. Three values were used:

$\sigma = 0.5$
$\sigma = 1$ (base case)
$\sigma = 2$

The figure shows that results for the base case are comparable to those for $\sigma = 2$, but are higher (thus more conservative) than those for $\sigma = 0.5$.

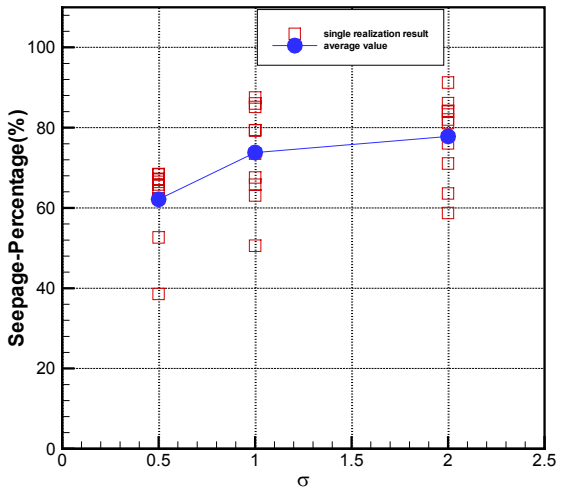

Output - DTN: LB0304SMDCREV2.002

Figure 6-13. Seepage Percentage as a Function of Standard Deviation σ, with $\log_{10} k_{FC} = -12$, $Q_p = 200$ mm/yr, $1/\alpha = 600$ Pa

6.6.3 Results for Degraded-Drift Scenario

As described in Section 6.4, the calculated drift-degradation profiles (see Section 5) are used. Figure 6-14 (a) shows two vertical sections of the discretized profiles matching the case of 75 percentile of drift degradation in the Tptpmn unit (Section 5). The 75 percentile means that 75% of the cases calculated in the drift-degradation simulation have smaller fall-off volume than this case. The normal drift profile without degradation is shown in Figure 6-14(b) for comparison. The color contours in this figure show the calculated liquid saturation distribution for Q_p= 200 mm/yr. Degradation created a more square-like profile (left profile in Figure 6-14a), which creates less flow diversion than a smooth circular profile. One can therefore see a slightly larger area of high saturation near this location. Figure 6-15 presents the seepage rates for a range of Q_p for this case. Results of seepage percentage for ten realizations of the degraded drift for the model (with cross-sectional area of 6.706 m^2, see Section 6.3.1, first paragraph) are shown as red squares in the figure. Note that the rock-fall is at about the middle of this model domain. To obtain the mean seepage over the drift containing one waste canister (with area of 28.05 m^2, see Section 6.3.1, first paragraph), one needs to recognize that the extra area 28.05 – 6.706 = 21.344 m^2 (i.e., the area of drift minus the area of the part of the drift containing the rock-fall) does not contain rock-fall. Since the mean seepage without drift degradation has been calculated (blue filled circles in Figure 6-15), one can calculate the mean seepage with degradation by combining the calculated seepage with and without degradation in the ratio of 6.706 to 21.344. The results are shown as black open circles in Figure 6-15. It turns out that the mean for the degraded case has actually slightly less seepage, though the geostatistical spread is quite large.

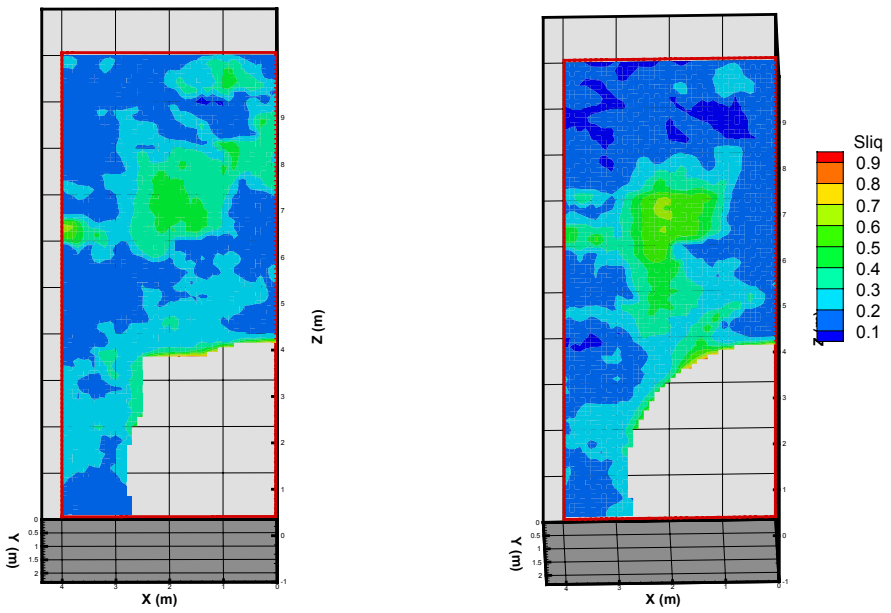

(a) (b)

Output-DTN: LB0304SMDCREV2.002

Figure 6-14. Liquid Saturation (Sliq) Distribution for the 75 Percentile Case Profile in Tptpmn Unit (left) and No-Degradation Base Case (right) ($\log_{10} k_{FC}$ = –11.86, Q_p = 200 mm/yr, $1/\alpha$ = 600 Pa)

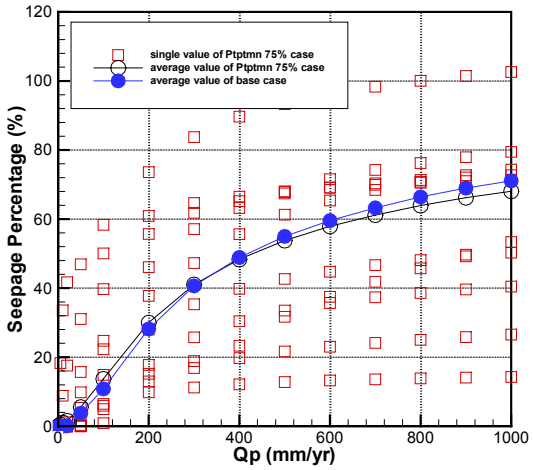

Output - DTN: LB0304SMDCREV2.002

Figure 6-15. Seepage Percentage as a Function of Percolation Flux for the 75 Percentile Case Profile in Tptpmn Unit ($\log_{10} k_{FC}$ = –11.86, $1/\alpha$ = 600 Pa). Red open squares are results for 10 realizations. The mean seepage percentages are shown as black open circles (see Text). For comparison, the mean over 10 realizations for no-degradation case (base case) is shown as blue filled circles.

Similar results for the worst-case drift-degradation profile (Section 5) are shown in Figure 6-16 and 6-17, for the Tptpmn unit. In this case, however, the rock-fall is extensive and is located at the center above the drift crown, thus cutting across the model boundary. The rock-fall volume is scaled accordingly, so that the mean seepage does not need to be scaled as in the case of Figure 6-15. The results of mean seepage percentages for degraded cases are shown as black open circles in Figure 6-17. They show small changes in seepage percentage (Figure 6-17) compared to the geostatistical spread due to multiple realizations.

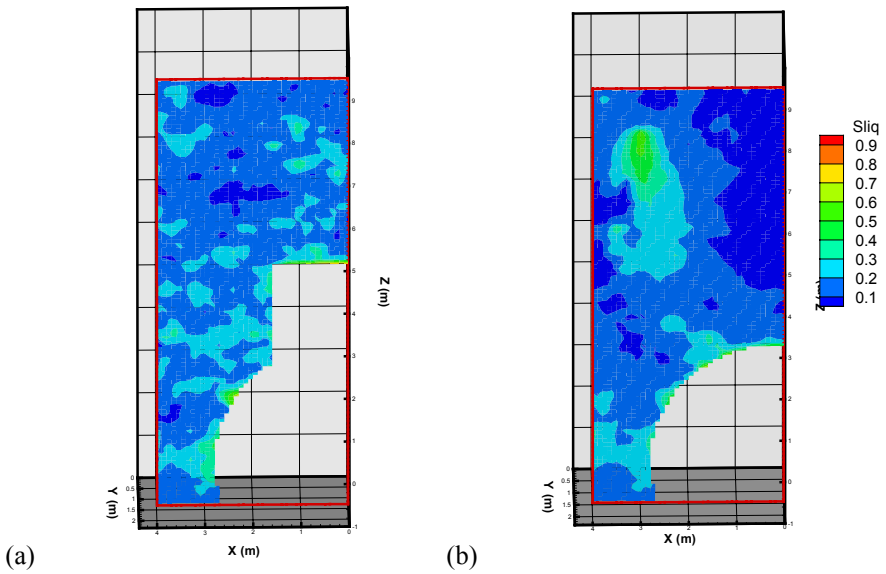

Output - DTN: LB0304SMDCREV2.002

Figure 6-16. Liquid Saturation (Sliq) Distribution for the Worst-Case Profile in Tptpmn Unit (left) and No-Degradation Base Case (right) ($\log_{10} k_{FC}$ = –11.86, Q_p = 200 mm/yr, $1/\alpha$ = 600 Pa)

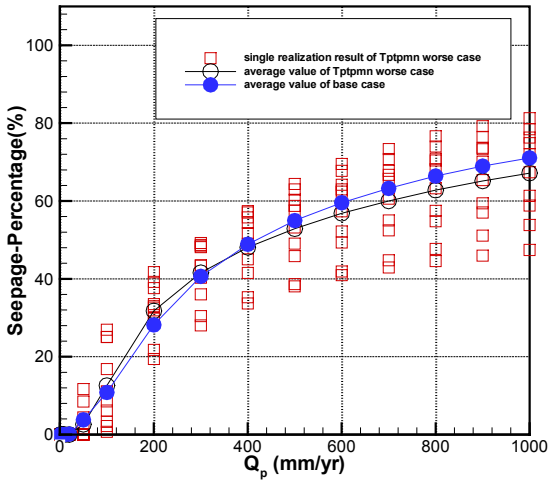

Output - DTN: LB0304SMDCREV2.002

Figure 6-17. Seepage Percentage as a Function of Percolation Flux for the Worst-Case Profile Case in Tptpmn Unit ($\log_{10} k_{FC} = -11.86$, $1/\alpha = 600$ Pa). Red open squares are the results for 10 realizations, with their mean shown as black open circles. For comparison, the mean over 10 realizations for the no-degradation case (base case) is shown as blue filled circles.

Corresponding results for the Tptpll unit are shown in Figures 6-18 to 6-21. For Figure 6-18 and 6-19 for the 75-percentile case, the rock-fall is located at the center above the drift crown and, since the model domain contains half the drift, only half of the rock-fall volume is used. Using a similar argument as above for results in Figure 6-15, the mean of seepage over the realizations with drift degradation is obtained by weighting the calculated seepage with and without degradation by the ratio $2 \times 6.706 = 13.412$ and $28.05 - 13.412 = 14.638$. The results are shown as black open circles in Figure 6-19. Then, for Figures 6-20 and 6-21 for the worst case, the rock-fall is located at about the middle of the model domain. Following the argument above related to Figure 6-15, the mean seepage percentages for the degraded drift were then calculated accordingly and are shown in Figure 6-21.

For both cases, the mean seepage for the degraded drift is somewhat higher than that of the nondegraded case. However, once again the geostatistical spread among the 10 realizations is much larger than this difference. For the 75-percentile case (Figure 6-19), nine realizations are bunched quite closely together (still spreading wider than the differences between the degraded and nondegraded cases), but one realization provides a larger seepage percentage. This is considered to be a geostatistically special case. Note that in the numerical results, in all cases, the seepage thresholds for both Tptpmn and Tptpll units appear not to have been significantly affected by drift degradation.

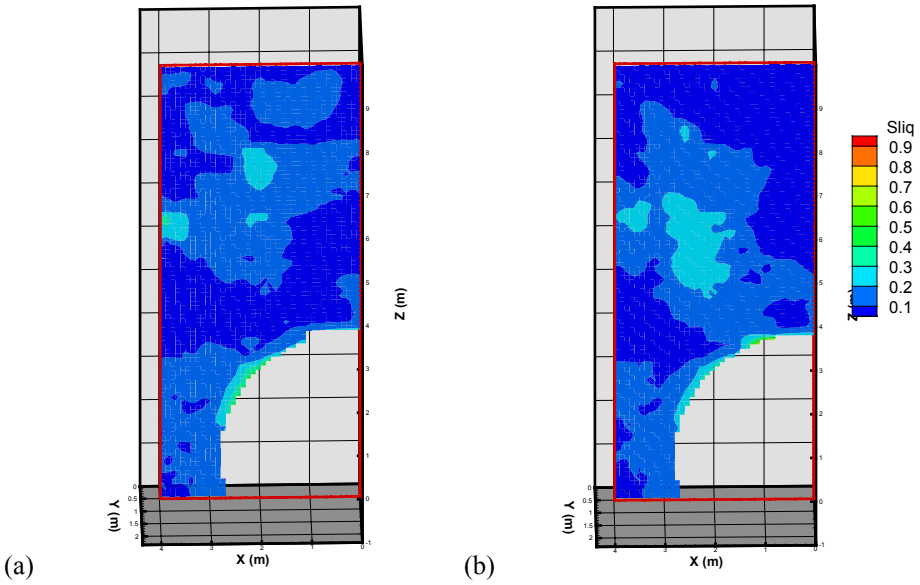

Output - DTN: LB0304SMDCREV2.002

Figure 6-18. Liquid Saturation (Sliq) Distribution for the 75 Percentile Case Profile in Tptpll Unit (left) and No-Degradation Base Case (right) ($\log_{10} k_{FC} = -10.84$, $Q_p = 200$ mm/yr, $1/\alpha = 600$ Pa).

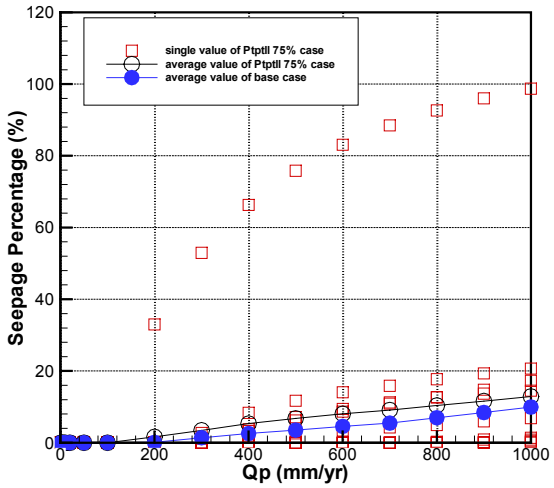

Output - DTN: LB0304SMDCREV2.002

Figure 6-19. Seepage Percentage as a Function of Percolation Flux for the 75 Percentile Case Profile in Tptpll Unit ($\log_{10} k_{FC} = -10.84$, $1/\alpha = 600$ Pa). Red open squares are results for 10 realizations. The mean seepage percentages are shown as black open circles (see text). For comparison, the mean over 10 realizations for no-degradation case (base case) is shown as blue-filled circles.

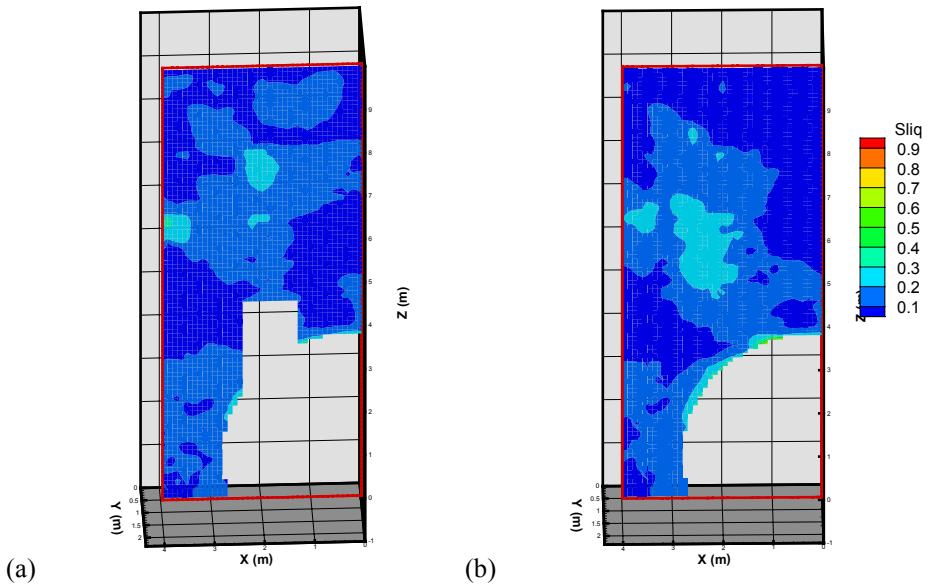

Output - DTN: LB0304SMDCREV2.002

Figure 6-20. Liquid Saturation (Sliq) Distribution for the Worst-Case Profiles in Tptpll Unit (left) and No-Degradation Base Case (right) ($\log_{10} k_{FC} = -10.84$, $Q_p = 200$ mm/yr, $1/\alpha = 600$ Pa)

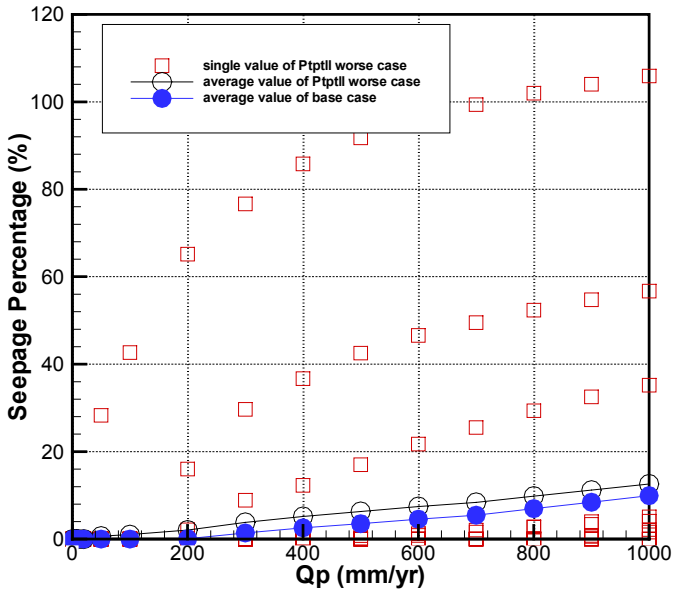

Output - DTN: LB0304SMDCREV2.002

Figure 6-21. Seepage Percentage as a Function of Percolation Flux for the Worst-Case Profiles in Tptpll Unit ($\log_{10} k_{FC} = -10.84$, $1/\alpha = 600$ Pa). Red open squares are results for 10 realizations. The mean seepage percentages are shown as black open circles (see text). For comparison, the mean over 10 realizations for no-degradation case (base case) is shown as blue filled circles.

6.6.4 Results for the Effect of Rock Bolts

Modeling results for seepage enhancement caused by the presence of a vertical rock bolt are shown in Table 6-4. Here, a seepage enhancement factor is defined as:

$$\text{Enhancement Factor} = 1 - \frac{SeepageWithTheRockbolts}{SeepageWithoutTheRockbolts} \qquad \text{Eq. (6.6-1)}$$

Thus, the enhancement factor is negative if the seepage increases because of the presence of a rock bolt and is positive if it decreases. Table 6-2 shows results only for Q_p = 500 mm/yr because, with Q_p = 5 mm/yr, seepage rates in all cases are zero, and enhancements are also found to be zero. In Table 6-2, Cases C1, C2 and C3 represent three variations in mesh design for accounting connections between rock-bolt borehole and the rock, and Cases G1 and G2 represent, respectively, the properties of grout being slightly degraded from original values and being very degraded, so that the rock-bolt hole is essentially open.

From the table, one can see that seepage enhancement is negligible for the presence of the rock bolt for the two limiting cases G1 and G2. This result is understandable, considering that the cross-sectional area of the rock-bolt borehole, onto which flow may be incident, is small, and the borehole can exchange moisture with the rock along its length. For a vertical rock bolt, if only the horizontal surface is considered, the area is only about 0.002 m^2. For a nonvertical rock bolt, while the area of rock bolt projected onto a horizontal plane is larger, the potential for flow from the rock-bolt borehole to the rock matrix around it is also increased.

Also note that the results are not sensitive to the alternative mesh design, C1, C2, and C3. Further, since the changes are so small, even the presence of five or six rock bolts will not change seepage significantly.

Table 6-4. Results on Seepage Enhancement Factor Due to a Rock Bolt in Drift Ceiling

1/α (Rock) Pa	Seepage Percentage (without rock bolt)	Seepage Enhancement Factor, Eq. 6.6-1 (with rock bolt)		
			Case G1 log k (grout) = –18 1/α (grout) = 10^7 Pa	Case G2 log k (grout) = –10 1/α (grout) = 10 Pa
200	100%	C1 C2 C3	0 0 0	0 0 0
400	53%	C1 C2 C3	0 0 0	0 0 0
589	0.034%	C1 C2 C3	–0.0033 –0.0113 –0.0156	–0.0034 –0.0113 –0.0156

Output - DTN: LB0304SMDCREV2.001

6.7 COMMENT ON LONG-TERM THC AND THM EFFECTS ON SEEPAGE

Long-term coupled thermal-hydrological-chemical (THC) processes have been modeled (BSC 2003 [163506]). Results from this modeling indicate a zone of permeability reduction corresponding to the boundary between the dryout zone near the drift and the condensation region farther away. Their calculations (BSC 2003 [163506], Section 6.8, Figures 6.8-40 and 6.8-41) show that the reduction is in the form of a circular shell between 5 and 7 m, or farther, from the drift ceiling. Thus, it acts as a shield to divert water around the drift, so that the drift sees relatively less percolation flux. As explained in Section 6.2, the drift, acting as a capillary barrier, diverts water around it and, where it is unable to do so fast enough, water accumulates, saturation increases, and seepage into drift occurs. However, all these processes act well within 1 m from the drift ceiling and drift wall (Philip et al. 1989 [105743]), and are not affected by these THC changes. Consequently, an alternative model with THC at long term is not considered.

The impact of long-term coupled thermal-hydrological mechanical (THM) processes has also been investigated (BSC 2003 [163501]). The results (BSC 2003 [163501], Section 6.4.4) show a thermally induced increase (by approximately a factor of 10) in horizontal permeability at 10,000 years, with a decrease in vertical permeability (also by approximately a factor of 10), in the immediate neighborhood (within 1 m) of the drift ceiling. This actually increases the likelihood of flow being diverted around the drift, and the changes are within the parameter ranges used in this Model Report. To confirm this point, calculations for Tptpmn were conducted within the THM modeling (BSC 2003 [163501]) using the permeability field after excavation with only mechanical effects (BSC 2003 [163501], Figure 6.5.1-1) and the permeability field at 10,000 year with THM effects (BSC 2003 [163501], Figure 6.5.4-3(d), Figure 6.5.4-4 (d)). Percolation flux was imposed above the drift with a series of values. The $1/\alpha$ value just above the drift crown after excavation was set to be 604.3 Pa (DTN: LB0302SCMREV02.002 [162273]). Seepage percentages were calculated (Wang 2003 [162319], SN-LBNL-SCI-204-V2, p. 162) and shown in Figure 6-22. The reduced seepage for the THM case at 10,000 years is apparent. Thus, an alternative model capturing THM long-term effects is not considered.

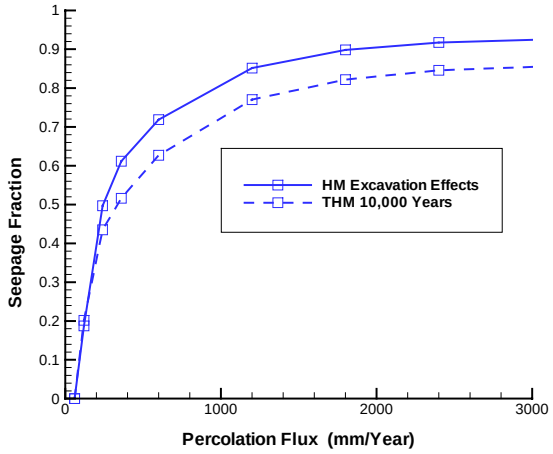

Output-DTN: LB0304SMDCREV2.004 (Attachment I, Table I-3)

Figure 6-22. Seepage Percentage (Expressed in Fraction) Is Shown as a Function of Percolation Flux for Permeability Fields around the Drift after Excavation and Also at 10,000 Years, Accounting for THM Effects

6.8 ALTERNATIVE CONCEPTUAL MODELS AND SENSITIVITY ANALYSIS

The main alternative conceptual model is the discrete fracture-network model (DFNM). This has been thoroughly discussed in BSC (2003 [162267], Section 6.4.1) and will not be repeated here (see also Section 6.3 of this Model Report). The results of the discussions in BSC (2003 [162267], Section 6.4.1) may be summarized as follows. The development of a defensible DFNM requires collecting a very large amount of geometric and hydrological data from the fracture network, which are mostly unavailable. Moreover, unsaturated hydrological parameters on the scale of individual fractures are required, along with conceptual models and simplifying assumptions regarding unsaturated flow within fractures and across fracture intersections. Thus, the parsimony of the continuum model is considered a key advantage over the complexity of the DFNM, which is difficult to support or justify in spite of its visual appeal. Moreover, a 2-D DFNM is not capable of capturing flow diversion within the fracture plane, a mechanism appropriately represented by a 2-D (or 3-D) continuum model. Hence, the full development of a DFNM as a potential alternative to the base-case continuum model is considered unwarranted.

Another alternative conceptual model is that of a drift in a homogeneous constant-property medium (Philip et al. 1989 [105743], pp. 17–21). Seepage into drift under conditions discussed in this Model Report is controlled by heterogeneity-induced channeling and local ponding (Birkholzer et al. 1999 [105170], pp. 358–384), which occurs much earlier than if the medium is homogeneous. In other words, the homogenous, constant-property model would predict seepage to occur at a threshold that is orders of magnitude larger. In this sense, Philip's approach is not relevant, and Philip's boundary-layer-flow regime near the drift crown (Philip et al. 1989 [105743], p. 21, Figure 1) should not be used to define the required grid size. Note that in this Model Report, the same conceptual approach and the same level of grid refinement as in the SCM are used. The calibration procedure accounts for the selected grid size by matching results with field data.

Another possible alternative could be a 2-D conceptual model. However, the drift seepage problem involves the accumulation of unsaturated flow at the location near the drift wall. This accumulation continues until the local saturation is large and capillary suction is small. Then seepage into drift occurs. This problem is intrinsically a 3-D problem, because flow accumulation at a location in 2-D could easily disappear if it is allowed to flow away in the third dimension. Two-dimensional models would consequently overestimate seepage.

The present Model Report considers spatial correlation lengths using a spherical correlation structure and a Gaussian field. There have been suggestions to use alternative geostatistical methods, such as nonparametric representations of the heterogeneity field and multiple-scale correlation structures. However, for a specific problem with a particular scale of a drift, such complications are not needed so long as the parameters used are appropriate to this scale.

The above discussions cover uncertainty related to the conceptual model. The continuum model is considered the best model for the SMPA not only because of these discussions, but also because it makes the SMPA consistent with the SCM (BSC 2003 [162267]), which has gone through calibration and validation against field data and observation. This adds confidence to the SMPA.

Concerning parameter uncertainty, the Model Report has made a comprehensive study by conducting Monte Carlo simulations on seepage into drift over wide ranges of parameters covering uncertainties in flow fields and rock properties. The sensitivity of different parameters is an integral part of the results and analysis presented in Section 6.6. It is recognized that parameter uncertainty is different from parameter variability. The latter is represented by the σ and λ parameters discussed in Section 6.3.3 and 6.3.5; the sensitivity of seepage on those parameters is discussed in Section 6.6.2.

Uncertainty associated with geostatistics (i.e., different realizations corresponding to the same input parameters of k_{FC}, σ, and λ) is evaluated through calculations of 20 realizations for each case (10 for sensitivity studies). In general, establishing geostatistical probability can require more realizations than 20, but the great number of 3-D simulations in this Model Report make it impractical to do more realizations. Nevertheless, the spread of results from the 20 realizations should give an indication of geostatistical variation.

7. VALIDATION

Validation of a model normally requires testing model results against relevant data not used in the original model development. For the Seepage Model for PA, these data should include seepage flux under low-percolation conditions over periods of years, even hundreds of years, at many locations in the repository block (for proper statistical representation). No such data are available. Further, data for adequate validation would need to cover the wide range of conditions studied in this Model Report. Those are not available either. This lack of data has necessitated the use of alternative approaches for model validation as described in Section 5.4.1 of AP-SIII.10Q, *Models*. In accordance with requirements of Section 5.4.1(b) of AP-SIII.10Q, confidence building during development of the SMPA has included establishment of wide ranges of key parameters affecting seepage, namely fracture continuum permeability, capillary strength, and percolation flux. The sensitivity of seepage results to these and other parameters has been evaluated. It was determined from these evaluations that expected changes in permeability as a result of potential irreversible THM and THC processes (BSC 2003 [163501] and BSC 2003 [163506]) are within the range of fracture-continuum permeability investigated in this Model Report.

Consistent with TWP (BSC 2002 [160819], Attachment I, Section I-4-2-1), postdevelopment model validation activities were performed by at least one of the methods listed in AP-SIII.10Q, Section 5.4.1 (c). Specifically, the following method has been used:

7.1 CORROBORATION WITH ALTERNATIVE MATHEMATICAL MODELS

With this method, a careful comparison is made of the SMPA results with the SCM (BSC 2003 [162267]), which has gone through calibration and validation against field data and observations. It is to be noted that the SCM is designed to simulate field tests in niches and boreholes with point liquid release, and the SMPA is designed for long-term steady-state simulations of seepage into drifts with percolation flux spread over the upper boundary of flow domain. As such, they are different. According to TWP (BSC 2002 [160819]), results from the SMPA are to be compared with those of the SCM (BSC 2003 [162267]) for a particular case. Agreement of the results within 20% will be the criterion for accepting the SMPA as having been validated sufficiently for the purpose of LA. The SCM calculations were carried out for the case of SYBT-ECRB-LA#2 (BSC 2003 [162267], Section 6.6.2.2), using a range of permeability, capillary, and percolation flux values on ten realizations of the heterogeneous field generated for the SCM (Wang 2003 [162319], SN-LBNL-SCI-228-V1, pp. 38–41). The results are presented in Table 7-1. In this table, the first three columns indicate the many cases with different parameter values of ($\log k$, $1/\alpha$, Q_p), for which the simulations were performed. The fourth column gives the mean over 10 realizations of the seepage percentage, calculated by the SCM, using the definition of seepage percentage in this Model Report (Section 6.6). In the SCM, the drift diameter is 5 m, slightly different from the drift diameter of 5.5 m used in the SMPA, and $\lambda = 0.2$ m as compared with $\lambda = 0.3$ m in the SMPA. The SCM results are compared with those of the SMPA (the fifth column in Table 7-1), taken from Section 6.6.1, which are the mean seepage percentages calculated from results using 20 realizations of the heterogeneous permeability field generated for the SMPA. Differences are on the order of 2% or less, and this meets the criterion

for accepting the SMPA as having been validated sufficiently for the purpose of LA. This is strong support for the SMPA.

Table 7-1. Comparison between Mean Seepage Percentages of the SMPA (20 Realizations) and the SCM (10 Realizations)

log(k)	1/α	Q_p	Seepage % SCM (mean over 10 realizations)	Seepage % SMPA (mean over 20 realizations)	SMPA % – SMC %
–13.00	200.00	200.00	99.28	98.64	–0.64
–12.00	200.00	200.00	96.43	95.43	–1.00
–11.00	200.00	200.00	85.49	83.86	–1.63
–13.00	400.00	200.00	92.15	90.79	–1.36
–12.00	400.00	200.00	70.17	68.65	–1.52
–11.00	400.00	200.00	14.01	14.55	0.54
–13.00	600.00	200.00	79.73	77.87	–1.86
–12.00	600.00	200.00	31.70	30.97	–0.73
–11.00	600.00	200.00	0.01	0.00	–0.01
–13.00	200.00	500.00	99.67	99.16	–0.51
–12.00	200.00	500.00	98.06	97.26	–0.80
–11.00	200.00	500.00	91.43	89.98	–1.45
–13.00	400.00	500.00	95.68	94.88	–0.80
–12.00	400.00	500.00	82.37	80.63	–1.74
–11.00	400.00	500.00	39.36	38.09	–1.27
–13.00	600.00	500.00	88.12	86.62	–1.50
–12.00	600.00	500.00	56.28	54.40	–1.88
–11.00	600.00	500.00	2.94	3.14	0.20
–13.00	200.00	800.00	99.92	99.47	–0.45
–12.00	200.00	800.00	98.60	97.88	–0.72
–11.00	200.00	800.00	93.58	92.26	–1.32
–13.00	400.00	800.00	96.92	96.41	–0.51
–12.00	400.00	800.00	86.45	84.84	–1.61
–11.00	400.00	800.00	52.06	50.11	–1.95
–13.00	600.00	800.00	91.15	90.02	–1.13
–12.00	600.00	800.00	65.74	64.33	–1.41
–11.00	600.00	800.00	8.61	9.15	0.54

Output - DTN: LB0304SMDCREV2.002

7.2 INDEPENDENT TECHNICAL REVIEW

For corroboration, the SMPA has also been published in the open scientific literature (Birkholzer et al. 1999 [105170], pp. 349–384; and Li and Tsang 2003 [163714]), having gone through anonymous technical review and public scientific scrutiny. Furthermore, the basic formulations of physical processes implemented in the SMPA, as represented by Richards' equation (Richards 1931 [104252], pp. 318–333), the van Genuchten-Mualem model (Luckner et al. 1989 [100590], pp. 2191–2192), Philip's studies (Philip et al. 1989 [105743], pp. 16–28), and effects of flow channeling resulting from heterogeneity and ponding (Birkholzer and Tsang 1997 [119397], pp. 2221–2224; Birkholzer et al. 1999 [105170], pp. 370–379), are all in the open literature, have gone through proper technical review, and have withstood scrutiny of the scientific community since their dates of publication.

With the exception of confirming the assumption in Section 5, no further activities are needed to complete this model validation before LA for its intended use.

INTENTIONALLY LEFT BLANK

8. CONCLUSIONS

The present Model Report is based on the SCM (BSC 2003 [162267]) and a review of available *in situ* field data appropriate to the Tptpmn and the Tptpll. The model has been previously described in Birkholzer et al. (1999 [105170]). The FEPs in Table 6-2 are addressed in this model. In reviewing available information (Sections 6.3 to 6.5), ranges of parameters were selected, over which seepage calculations were conducted. All eight items in the work scope in Section 1 have been accomplished: the SMPA has been developed, parameter ranges selected, simulations designed and performed, drift-collapse results reviewed, degradation profiles constructed (and simulations performed accordingly), and impact of rock bolts evaluated. Finally, these results are in partial support of FEP evaluation, as discussed in Section 6.2.1.

The results (Figures 6-4 to 6-21) show the impact of various factors on seepage, and calculated data are provided to TDMS for PA to develop probability distributions. Generally, seepage is found to be larger for smaller fracture continuum permeability (k_{FC}), smaller van Genuchten parameter ($1/\alpha$) and larger percolation flux (Q_p) values. This is very reasonable, since a small k_{FC} reduces flow diversion around the drift, and a small $1/\alpha$ parameter represents a small capillary strength and thus a small capillary barrier effect. In addition, a larger Q_p provides more water into the system to induce higher seepage. These results form a useful data set for model abstraction for TSPA.

The acceptance criteria listed in Section 4.2 are met by the present Model Report, as explained below.

For those identified under Section 2.2.1.3.3.3 of the YMRP (NRC 2003 [162418]):

- Acceptance Criterion 1, *System Description and Model Integration Are Adequate*:

  The physics of the seepage phenomenon is adequately incorporated into the SMPA based on a sufficient technical basis, supported by field data and sensitivity analyses, through the SCM (on which the SMPA is based). See Sections 6.2 and 6.3.

- Acceptance Criterion 2, *Data Are Sufficient for Model Justification*:

  Ranges of hydrological values used are adequately justified and described. Sufficient ranges are used for seepage simulations needed for the Seepage Abstraction Model. See Sections 6.3.2 through 6.3.7.

- Acceptance Criterion 3, *Data Uncertainty Is Characterized and Propagated through the Model Abstraction*

  The parameters and their ranges are used in simulations to cover data uncertainties and variabilities (Section 6.3.2 to 6.3.7). The results are provided to the Seepage Abstraction Model as a comprehensive look-up table for easy use and traceability.

- Acceptance Criterion 4, *Model Uncertainty Is Characterized and Propagated through the Model Abstraction*:

The selected modeling approach is consistent with the SCM and current scientific understanding. Alternative models have been discussed (see Section 6.8). Results cover uncertainties of parameter ranges from the SCM and other sources. These are propagated as tables with results of both mean and standard deviations, to be used in Model Abstraction.

For those identified under Section 2.2.1.1.3 of the YMRP (NRC 2003 [162418]):

- Acceptance Criterion 1, *Identification of Barriers is Adequate:*

  Barriers are adequately identified and linked to their capability. The discussion is found in Section 6.2.

  Acceptance Criterion 2, *Description of Barrier Capability to Isolate Waste is Acceptable:*

  The capability of the barrier to prevent or substantially reduce the rate of movement of water is consistent with the definition of a barrier in 10 CFR 63 [156605], Section 63.2 and is adequately identified and described, including the uncertainty associated with the barrier's capability. See Section 6.2 and 6.6.

  Acceptance Criterion 3, *Technical Basis for Barrier Capability is Adequately Presented:*

  The technical basis for assertions of barrier capability is commensurate with the importance of the barrier's capability and the associated uncertainties. See Section 6.3.

8.1 LIMITATIONS

The results in this Model Report are based on current repository design, on available site data, and on the SCM (BSC 2003 [162267]), and are dependent on the continuum conceptual model. Further, this model report is on ambient conditions. Transient short-term THC and THM effects are not considered. Application of results should be within these limits.

This report demonstrates that the impact of mechanical effects such as rock-falls and fracture dilation can be evaluated (Sections 6.4 and 6.5). This work builds on BSC 2001 [156304], which includes fracture-dilation scoping analyses. These reports also considered thermal and seismic effects on drift degradation in a schematic way. As further mechanical studies are made on drift degradation, seepage calculations should follow to provide an assessment of their impact.

Reasonable changes in the input data used to establish ranges of parameter values used in this Model Report would not affect the choice of these ranges. For example, the permeability data are used to establish a range of values for the simulations. These permeability data could change by an order of magnitude, yet still be within the selected range and not affect the sets of results. On the other hand, smaller diameter drifts would generally result in less seepage.

8.2 RECOMMENDATIONS

As new data or upstream modeling results become available, they should be examined to assess their impact on seepage. In particular, the Model Report uses the calculated drift-degradation

profiles from BSC (2001 [156304]); see Section 5. As results from on-going drift degradation studies are available, seepage calculation should follow, so that the assumption of using currently available degradation profiles can be confirmed.

8.3 DEVELOPED DATA

Data developed in the current Model Report have been submitted to TDMS and their DTNs are listed below and in Section 9.4.

LB0304SMDCREV2.001

LB0304SMDCREV2.002

LB0304SMDCREV2.003

LB0304SMDCREV2.004

Descriptions of these files are given in Attachment I. The first file gives output data for all the simulation runs for all cases and all realizations. The second file gives summary results, which are also presented as figures in Section 6.6. These two data files are to be used in the upcoming revision of *Abstraction of Drift Seepage* (CRWMS M&O 2001 [154291]) for TSPA-LA. The last two data files are in support of discussions in the present Model Report only. They are, respectively, files for calculating THM effects on seepage and files for plotting the results, presented in Section 6.7.

INTENTIONALLY LEFT BLANK

9. INPUTS AND REFERENCES

The following is a list of the references cited in this document. Column 1 represents the unique six digit numerical identifier (the Document Input Reference System [DIRS] number), which is placed in the text following the reference callout (e.g., BSC 2002 [160819]). The purpose of these numbers is to assist the reader in locating a specific reference. Within the reference list, multiple sources by the same author (e.g., BSC 2002) are sorted alphabetically by title.

9.1 DOCUMENTS CITED

119397 Birkholzer, J. and Tsang, C.F. 1997. "Solute Channeling in Unsaturated Heterogeneous Porous Media." *Water Resources Research, 33*, (10), 2221-2238. Washington, D.C.: American Geophysical Union. TIC: 235675.

105170 Birkholzer, J.; Li, G.; Tsang, C-F.; and Tsang, Y. 1999. "Modeling Studies and Analysis of Seepage into Drifts at Yucca Mountain." *Journal of Contaminant Hydrology, 38*, (1-3), 349-384. New York, New York: Elsevier. TIC: 244160.

119404 Brekke, T.L.; Cording, E.J.; Daemen, J.; Hart, R.D.; Hudson, J.A.; Kaiser, P.K.; and Pelizza, S. 1999. *Panel Report on the Drift Stability Workshop, Las Vegas, Nevada, December 9-11, 1998*. Las Vegas, Nevada: Management and Technical Support Services. ACC: MOL.19990331.0102.

156304 BSC (Bechtel SAIC Company) 2001. *Drift Degradation Analysis*. ANL-EBS-MD-000027 REV 01 ICN 01. Las Vegas, Nevada: Bechtel SAIC Company. ACC: MOL.20011029.0311.

155187 BSC (Bechtel SAIC Company) 2001. *Ground Control for Emplacement Drifts for SR*. ANL-EBS-GE-000002 REV 00 ICN 01. Las Vegas, Nevada: Bechtel SAIC Company. ACC: MOL.20010627.0028.

160798 BSC (Bechtel SAIC Company) 2002. *Repository Design Project, Repository/PA IED Emplacement Drift Configuration*. 800-IED-EBS0-00200-000-00A. Las Vegas, Nevada: Bechtel SAIC Company. ACC: MOL.20021031.0104.

160317 BSC (Bechtel SAIC Company) 2002. *Repository Design Project, Repository/PA IED Typical Waste Package Components Assembly*. 800-IED-EBS0-00100-000-00A. Las Vegas, Nevada: Bechtel SAIC Company. ACC: MOL.20021015.0310.

161067 BSC (Bechtel SAIC Company) 2002. *Requirements Document (RD) for iTOUGH2 V5.0-00*. DI: 10003-RD-5.0-0. Las Vegas, Nevada: Bechtel SAIC Company. ACC: MOL.20020923.0143.

160819 BSC (Bechtel SAIC Company) 2002. *Technical Work Plan for: Performance Assessment Unsaturated Zone*. TWP-NBS-HS-000003 REV 02. Las Vegas, Nevada: Bechtel SAIC Company. ACC: MOL.20030102.0108.

161066 BSC (Bechtel SAIC Company) 2002. *User's Manual (UM) for iTOUGH2 V5.0*. DI: 10003-UM-5.0-00. Las Vegas, Nevada: Bechtel SAIC Company. ACC: MOL.20020923.0147.

161773 BSC (Bechtel SAIC Company) 2003. *Analysis of Hydrologic Properties Data*. MDL-NBS-HS-000014 REV 00. Las Vegas, Nevada: Bechtel SAIC Company. ACC: DOC.20030404.0004.

163501 BSC (Bechtel SAIC Company) 2003. *Drift Scale THM Model*. MDL-NBS-HS-000017 REV 00A. Las Vegas, Nevada: Bechtel SAIC Company. ACC: MOL.20030506.0239. TBV-5119

163506 BSC (Bechtel SAIC Company) 2003. *Drift-Scale Coupled Processes (DST and THC Seepage)*. MDL-NBS-HS-000001 REV 02C. Las Vegas, Nevada: Bechtel SAIC Company. ACC: MOL.20030507.0274. TBV-5120

162267 BSC (Bechtel SAIC Company) 2003. *Seepage Calibration Model and Seepage Testing Data*. MDL-NBS-HS-000004 REV 02. Las Vegas, Nevada: Bechtel SAIC Company. ACC: DOC.20030408.0004.

163840 BSC (Bechtel SAIC Company) 2003. *Technical Work Plan for: Engineered Barrier System Department Modeling and Testing FY03 Work Activities*. TWP-MGR-MD-000015 REV 04. Las Vegas, Nevada: Bechtel SAIC Company. ACC: DOC.20030616.0002.

161770 Canori, G.F. and Leitner, M.M. 2003. *Project Requirements Document*. TER-MGR-MD-000001 REV 01. Las Vegas, Nevada: Bechtel SAIC Company. ACC: DOC.20030404.0003.

154291 CRWMS M&O (Civilian Radioactive Waste Management System Management and Operating Contractor) 2001. *Abstraction of Drift Seepage*. ANL-NBS-MD-000005 REV 01. Las Vegas, Nevada: CRWMS M&O. ACC: MOL.20010309.0019.

153481 Cushey, M. 2000. Drift Scale Modeling (YMP-LBNL-DSM-MC-1). Scientific Notebook SN-LBNL-SCI-052-V1. ACC: MOL.20000824.0558.

151875 Finsterle, S. 2000. "Using the Continuum Approach to Model Unsaturated Flow in Fractured Rock." *Water Resources Research, 36*, (8), 2055-2066. [Washington, D.C.]: American Geophysical Union. TIC: 248769.

154365 Freeze, G.A.; Brodsky, N.S.; and Swift, P.N. 2001. *The Development of Information Catalogued in REV00 of the YMP FEP Database*. TDR-WIS-MD-000003 REV 00 ICN 01. Las Vegas, Nevada: Bechtel SAIC Company. ACC: MOL.20010301.0237.

141523 Jackson, C.P.; Hoch, A.R.; and Todman, S. 2000. "Self-Consistency of a Heterogeneous Continuum Porous Medium Representation of a Fractured Medium." *Water Resources Research, 36*, (1), 189-202. Washington, D.C.: American Geophysical Union. TIC: 247466.

154293 Knight, J.H.; Philip, J.R.; and Waechter, R.T. 1989. "The Seepage Exclusion Problem for Spherical Cavities." *Water Resources Research, 25*, (1), 29-37. [Washington, D.C.]: American Geophysical Union. TIC: 240851.

163714 Li, G. and Tsang, C-F. 2003. "Seepage into Drifts with Mechanical Degradation." *Journal of Contaminant Hydrology, 62-63*, 157-172. New York, New York: Elsevier. TIC: 254205.

100590 Luckner, L.; van Genuchten, M.T.; and Nielsen, D.R. 1989. "A Consistent Set of Parametric Models for the Two-Phase Flow of Immiscible Fluids in the Subsurface." *Water Resources Research, 25*, (10), 2187-2193. Washington, D.C.: American Geophysical Union. TIC: 224845.

162418 NRC (U.S. Nuclear Regulatory Commission) 2003. *Yucca Mountain Review Plan, Information Only*. NUREG-1804, Draft Final Revision 2. Washington, D.C.: U.S. Nuclear Regulatory Commission, Office of Nuclear Material Safety and Safeguards. TIC: 254002.

152651 Philip, J.R. 1989. "The Seepage Exclusion Problem for Sloping Cylindrical Cavities." *Water Resources Research, 25*, (6), 1447-1448. [Washington, D.C.]: American Geophysical Union. TIC: 239729.

105743 Philip, J.R.; Knight, J.H.; and Waechter, R.T. 1989. "Unsaturated Seepage and Subterranean Holes: Conspectus, and Exclusion Problem for Circular Cylindrical Cavities." *Water Resources Research, 25*, (1), 16-28. Washington, D.C.: American Geophysical Union. TIC: 239117.

104252 Richards, L.A. 1931. "Capillary Conduction of Liquids Through Porous Mediums." *Physics, 1*, 318-333. [New York, New York: American Physical Society]. TIC: 225383.

139174 Ritcey, A.C. and Wu, Y.S. 1999. "Evaluation of the Effect of Future Climate Change on the Distribution and Movement of Moisture in the Unsaturated Zone at Yucca Mountain, NV." *Journal of Contaminant Hydrology, 38*, (1-3), 257-279. New York, New York: Elsevier. TIC: 244160.

100610 van Genuchten, M.T. 1980. "A Closed-Form Equation for Predicting the Hydraulic Conductivity of Unsaturated Soils." *Soil Science Society of America Journal, 44*, (5), 892-898. Madison, Wisconsin: Soil Science Society of America. TIC: 217327.

162319 Wang, J.S. 2003. "Scientific Notebooks Referenced in Model Report U0075, Seepage Model for PA Including Drift Collapse, MDL-NBS-HS-000002 REV 02." Memorandum from J.S. Wang (BSC) to File, May 5, 2003, with attachments. ACC: MOL.20030506.0299.

106146 Wang, J.S.Y.; Trautz, R.C.; Cook, P.J.; Finsterle, S.; James, A.L.; and Birkholzer, J. 1999. "Field Tests and Model Analyses of Seepage into Drift." *Journal of Contaminant Hydrology, 38*, (1-3), 323-347. New York, New York: Elsevier. TIC: 244160.

117161 Wu, Y-S.; Haukwa, C.; and Bodvarsson, G.S. 1999. "A Site-Scale Model for Fluid and Heat Flow in the Unsaturated Zone of Yucca Mountain, Nevada." *Journal of Contaminant Hydrology, 38*, (1-3), 185-215. New York, New York: Elsevier. TIC: 244160.

Software Cited

134141 LBNL (Lawrence Berkeley National Laboratory) 1999. *Software Code: EXT*. V1.0. Sun. 10047-1.0-00.

153100 LBNL (Lawrence Berkeley National Laboratory) 2000. *Software Code: GSLIB*. V1.0SISIMV1.204. SUN w/Unix OS. 10397-1.0SISIMV1.204-00.

146496 LBNL (Lawrence Berkeley National Laboratory) 2000. *Software Code: TOUGH2*. V1.4. Sun Workstation and DEC/ALPHA. 10007-1.4-01.

152823 LBNL (Lawrence Berkeley National Laboratory) 2000. *Software Routine: AddBound*. V1.0. SUN w/Unix OS. 10357-1.0-00.

152816 LBNL (Lawrence Berkeley National Laboratory) 2000. *Software Routine: CutDrift*. V1.0. SUN w/Unix OS. 10375-1.0-00.

152828 LBNL (Lawrence Berkeley National Laboratory) 2000. *Software Routine: CutNiche*. V1.3. SUN w/Solaris OS. 10402-1.3-00.

152824 LBNL (Lawrence Berkeley National Laboratory) 2000. *Software Routine: MoveMesh*. V1.0. SUN w/Unix OS. 10358-1.0-00.

152826 LBNL (Lawrence Berkeley National Laboratory) 2000. *Software Routine: Perm2Mesh*. V1.0. SUN w/Unix OS. 10359-1.0-00.

160106 LBNL (Lawrence Berkeley National Laboratory) 2002. *Software Code: iTOUGH2*. V5.0. SUN UltraSparc., DEC ALPHA, LINUX. 10003-5.0-00.

9.2 CODES, STANDARDS, REGULATIONS, AND PROCEDURES

156605 10 CFR 63. Energy: Disposal of High-Level Radioactive Wastes in a Geologic Repository at Yucca Mountain, Nevada. Readily available.

AP-2.22Q, Rev. 0, ICN 1. *Classification Criteria and Maintenance of the Monitored Geologic Repository Q-List.* Washington, D.C.: U.S. Department of Energy, Office of Civilian Radioactive Waste Management. ACC: DOC.20030422.0009.

AP-SI.1Q, Rev. 5, ICN 0. *Software Management.* Washington, D.C.: U.S. Department of Energy, Office of Civilian Radioactive Waste Management. ACC: DOC.20030422.0012.

AP-SIII.10Q, Rev. 1, ICN 2. *Models.* Washington, D.C.: U.S. Department of Energy, Office of Civilian Radioactive Waste Management. ACC: DOC.20030627.0003.

9.3 SOURCE DATA, LISTED BY DATA TRACKING NUMBER

153155 LB0011AIRKTEST.001. Air Permeability Testing in Niches 3566 and 3650. Submittal date: 11/08/2000.

154586 LB0012AIRKTEST.001. Niche 5 Air K Testing 3/23/00-4/3/00. Submittal date: 12/21/2000.

159525 LB0205REVUZPRP.001. Fracture Properties for UZ Model Layers Developed from Field Data. Submittal date: 05/14/2002.

162277 LB0302PTNTSW9I.001. PTN/TSW Interface Percolation Flux Maps for 9 Infiltration Scenarios. Submittal date: 02/28/2003.

162273 LB0302SCMREV02.002. Seepage-Related Model Parameters K and 1/A: Data Summary. Submittal date: 02/28/2003.

163703 LB0304DRSCLTHM.001. Drift Scale THM Model Predictions: Simulations. Submittal date: 04/11/2003.

136593 LB980901233124.101. Pneumatic Pressure and Air Permeability Data from Niche 3107 and Niche 4788 in the ESF from Chapter 2 of Report SP33PBM4: Fracture Flow and Seepage Testing in the ESF, FY98. Submittal date: 11/23/1999.

104055 LB997141233129.001. Calibrated Basecase Infiltration 1-D Parameter Set for the UZ Flow and Transport Model, FY99. Submittal date: 07/21/1999.

156306 MO0109RDDAAMRR.003. Results from Drift Degradation Analysis. Submittal date: 09/24/2001.

161496 MO0301SEPFEPS1.000. LA FEP List. Submittal date: 01/21/2003.

9.4 OUTPUT DATA, LISTED BY DATA TRACKING NUMBER

LB0304SMDCREV2.001. Seepage Modeling for Performance Assessment, Including Drift Collapse: Input/Output Files. Submittal date: 04/11/2003.

LB0304SMDCREV2.002. Seepage Modeling for Performance Assessment, Including Drift Collapse: Summary Plot Files and Tables. Submittal date: 04/11/2003.

LB0304SMDCREV2.003. Impact of Thermal-Hydrologic-Mechanical Effects on Seepage: Simulations. Submittal date: 04/23/2003.

LB0304SMDCREV2.004. Impact of Thermal-Hydrologic-Mechanical Effects on Seepage: Summary Plot Files and Tables. Submittal date: 04/23/2003.

ATTACHMENT I—LIST OF COMPUTER FILES SUBMITTED WITH THIS MODEL REPORT UNDER OUTPUT-DTNS : LB0304SMDCREV2.001; LB0304SMDCREV2.002; LB0304SMDCREV2.003; LB0304SMDCREV2.004

Computer files used in this Model Report are listed below and are submitted to the TDMS under DTN: **LB0304SMDCREV2.001; LB0304SMDCREV2.002; LB0304SMDCREV2.003;** and **LB0304SMDCREV2.004.** Each file name is complemented with a short description of its contents and/or purpose. The detail could be found on the scientific notebook pages listed in Table 6-1.

Table I-1 lists the files of numerical simulations with the SMPA for three seepage-relevant parameters: fracture k, the capillary-strength, and percolation flux. Multiple realizations of the underlying stochastic permeability field are performed. Selected sensitivity analyses are performed on the effects of variable stages of drift collapse. Different design scenarios are modeled for rock-fall and rockbolt installations.

Table I-1. File Name and Description for Numerical Simulations **DTN: LB0304SMDCREV2.001**

File/Folder Name	Description
(Related to Sections 6.3 and 6.6)	
20_k-realizations/	
20_k-realizations/Tough2 mesh generation	
20_k-realizations/Tough2 mesh generation/Input/	
mesh3dblock	**TOUGH2 input file with MESHMAKER block**
20_k-realizations/Tough2 mesh generation/Output/	
mesh3dblock.mes	**TOUGH2 output file, mesh file**
SMPA	**TOUGH2 input file**
20_k-realizations/iTOUGH2 mesh generation/iT2 input/	
SMPA.mes1	Mesh with permeability realization #1
SMPA.mes2	Mesh with permeability realization #2
SMPA.mes3	Mesh with permeability realization #3
SMPA.mes4	Mesh with permeability realization #4
SMPA.mes5	Mesh with permeability realization #5
SMPA.mes6	Mesh with permeability realization #6
SMPA.mes7	Mesh with permeability realization #7
SMPA.mes8	Mesh with permeability realization #8
SMPA.mes9	Mesh with permeability realization #9
SMPA.mes10	Mesh with permeability realization #10
SMPA.mes11	Mesh with permeability realization #11
SMPA.mes12	Mesh with permeability realization #12
SMPA.mes13	Mesh with permeability realization #13
SMPA.mes14	Mesh with permeability realization #14
SMPA.mes15	Mesh with permeability realization #15
SMPA.mes16	Mesh with permeability realization #16
SMPA.mes17	Mesh with permeability realization #17
SMPA.mes18	Mesh with permeability realization #18
SMPA.mes19	Mesh with permeability realization #19
SMPA.mes20	Mesh with permeability realization #20
SMPAi	iTOUGH2 input file
Parameterset.dat	Input file for parameter combination

20_k-realizations/iTOUGH2 mesh generation/iT2 output/

SMPAi.out1	Seepage results for permeability realization #1
SMPAi.out2	Seepage results for permeability realization #2
SMPAi.out3	Seepage results for permeability realization #3
SMPAi.out4	Seepage results for permeability realization #4
SMPAi.out5	Seepage results for permeability realization #5
SMPAi.out6	Seepage results for permeability realization #6
SMPAi.out7	Seepage results for permeability realization #7
SMPAi.out8	Seepage results for permeability realization #8
SMPAi.out9	Seepage results for permeability realization #9
SMPAi.out10	Seepage results for permeability realization #10
SMPAi.out11	Seepage results for permeability realization #11
SMPAi.out12	Seepage results for permeability realization #12
SMPAi.out13	Seepage results for permeability realization #13
SMPAi.out14	Seepage results for permeability realization #14
SMPAi.out15	Seepage results for permeability realization #15
SMPAi.out16	Seepage results for permeability realization #16
SMPAi.out17	Seepage results for permeability realization #17
SMPAi.out18	Seepage results for permeability realization #18
SMPAi.out19	Seepage results for permeability realization #19
SMPAi.out20	Seepage results for permeability realization #20

20_k-realizations/iTOUGH2 mesh generation/pre-processing/

onestep	TOUGH2 input file to perform single time step simulation
perm.par	SISIM input file to generate heterogeneous log-permeability modifier field
Primary.mes	Primary mesh file
sh.mesh	Sequence of commands used to generate meshes for 20 realizations

(Related to Sections 6.5 and 6.6.4)
Rockbolt_analysis/

Rockboltsreadme.doc	Readme file for rockbolt simulation

Rockbolt_analysis/10cm_discrete_fracture_simulations/t21.5df1/

sh.22v1.4	Sequence of commands to run sensitivity study
vh_aX22	TOUGH2 input file (1/alpha =589 Pa)
vh_aX22.out	TOUGH2 output file
vh_aX22.seep	TOUGH2 output file

Rockbolt_analysis/10cm_discrete_fracture_simulations/t21.5df1_23/

sh.23v1.4	Sequence of commands to run sensitivity study
vh_aX23	TOUGH2 input file (1/alpha =400 Pa)
vh_aX23.out	TOUGH2 output file
vh_aX23.seep	TOUGH2 output file

Rockbolt_analysis/10cm_discrete_fracture_simulations/t21.5df1_24/

sh.24v1.4	Sequence of commands to run sensitivity study
vh_aX24	TOUGH2 input file (1/alpha =200 Pa)
vh_aX24.out	TOUGH2 output file
vh_aX24.seep	TOUGH2 output file

Rockbolt_analysis/50cm_discrete_fracture_simulations/t21.5df5/

sh.22v1.4	Sequence of commands to run sensitivity study
vh_aX22	TOUGH2 input file (1/alpha =589 Pa)
vh_aX22.out	TOUGH2 output file
vh_aX22.seep	TOUGH2 output file

Rockbolt_analysis/50cm_discrete_fracture_simulations/t21.5df5_23/

sh.23v1.4	Sequence of commands to run sensitivity study
vh_aX23	TOUGH2 input file (1/alpha =400 Pa)
vh_aX23.out	TOUGH2 output file
vh_aX23.seep	TOUGH2 output file

Rockbolt_analysis/50cm_discrete_fracture_simulations/t21.5df5_24/

sh.24v1.4	Sequence of commands to run sensitivity study
vh_aX24	TOUGH2 input file (1/alpha =200 Pa)
vh_aX24.out	TOUGH2 output file
vh_aX24.seep	TOUGH2 output file

Rockbolt_analysis/SCM_simulations/t21.5/

sh.22v1.4	Sequence of commands to run sensitivity study
vh_aX22	TOUGH2 input file (1/alpha =589 Pa)
vh_aX22.out	TOUGH2 output file
vh_aX22.seep	TOUGH2 output file

Rockbolt_analysis/SCM_simulations/t21.5_23/

sh.23v1.4	Sequence of commands to run sensitivity study
vh_aX23	TOUGH2 input file (1/alpha =400 Pa)
vh_aX23.out	TOUGH2 output file
vh_aX23.seep	TOUGH2 output file

Rockbolt_analysis/SCM_simulations/t21.5_24/

sh.24v1.4	Sequence of commands to run sensitivity study
vh_aX24	TOUGH2 input file (1/alpha =200 Pa)
vh_aX24.out	TOUGH2 output file
vh_aX24.seep	TOUGH2 output file

(Related to Section 7)
SMPA-SCMi/T2_input/

SMPA-SCM	TOUGH2 input file

SMPA-SCMi/T2_output-iT2_input/

SMPA-SCMi	iTOUGH2 input file
run_SMPA-SCM	Sequence of commands to run simulations

SMPA-SCMi/iT2_Output/

SMPA-SCMi.out1	Seepage results for permeability realization #1
SMPA-SCMi.out2	Seepage results for permeability realization #2
SMPA-SCMi.out3	Seepage results for permeability realization #3
SMPA-SCMi.out4	Seepage results for permeability realization #4
SMPA-SCMi.out5	Seepage results for permeability realization #5
SMPA-SCMi.out6	Seepage results for permeability realization #6
SMPA-SCMi.out7	Seepage results for permeability realization #7
SMPA-SCMi.out8	Seepage results for permeability realization #8
SMPA-SCMi.out9	Seepage results for permeability realization #9
SMPA-SCMi.out10	Seepage results for permeability realization #10

(Related to Sections 6.6.2 and 6.6.3)
k1-10_realizations_10-scenarios/

onestep	TOUGH2 input file to perform single time step simulation
sh.onestep	Sequence of command to run one time step

(Related to Section 6.6.2)
k1-10_realizations_10-scenarios/Sensitivity_analysis_4-scenarios/Common_input/

SMPAi	iTOUGH2 input file
parameterset1.dat	Input file for parameter combination

k1-10_realizations_10-scenarios/Sensitivity_analysis_4-scenarios/Correlation_length/lambda=1m/Input/

SMPAa1.mes1	Mesh with permeability realization #1
SMPAa1.mes2	Mesh with permeability realization #2
SMPAa1.mes3	Mesh with permeability realization #3
SMPAa1.mes4	Mesh with permeability realization #4
SMPAa1.mes5	Mesh with permeability realization #5
SMPAa1.mes6	Mesh with permeability realization #6
SMPAa1.mes7	Mesh with permeability realization #7
SMPAa1.mes8	Mesh with permeability realization #8
SMPAa1.mes9	Mesh with permeability realization #9
SMPAa1.mes10	Mesh with permeability realization #10
Perma1.par	SISIM input file to generate heterogeneous log-permeability modifier field
sh.mesha1	Sequence of commands used to generate meshes for 10 realizations

k1-10_realizations_10-scenarios/Sensitivity_analysis_4-scenarios/Correlation_length/lambda=1m/Output/

SMPAi.outa11	Seepage results for permeability realization #1
SMPAi.outa12	Seepage results for permeability realization #2
SMPAi.outa13	Seepage results for permeability realization #3
SMPAi.outa14	Seepage results for permeability realization #4
SMPAi.outa15	Seepage results for permeability realization #5
SMPAi.outa16	Seepage results for permeability realization #6
SMPAi.outa17	Seepage results for permeability realization #7
SMPAi.outa18	Seepage results for permeability realization #8
SMPAi.outa19	Seepage results for permeability realization #9
SMPAi.outa110	Seepage results for permeability realization #10

k1-10_realizations_10-scenarios/Sensitivity_analysis_4-scenarios/Correlation_length/lambda=2m/Input/

SMPAa2.mes1	Mesh with permeability realization #1
SMPAa2.mes2	Mesh with permeability realization #2
SMPAa2.mes3	Mesh with permeability realization #3
SMPAa2.mes4	Mesh with permeability realization #4
SMPAa2.mes5	Mesh with permeability realization #5
SMPAa2.mes6	Mesh with permeability realization #6
SMPAa2.mes7	Mesh with permeability realization #7
SMPAa2.mes8	Mesh with permeability realization #8
SMPAa2.mes9	Mesh with permeability realization #9
SMPAa2.mes10	Mesh with permeability realization #10
Perma2.par	SISIM input file to generate heterogeneous log-permeability modifier field
sh.mesha2	Sequence of commands used to generate meshes for 10 realizations

k1-10_realizations_10-scenarios/Sensitivity_analysis_4-scenarios/Correlation_length/lambda=2m/Output/

SMPAi.outa21	Seepage results for permeability realization #1
SMPAi.outa22	Seepage results for permeability realization #2
SMPAi.outa23	Seepage results for permeability realization #3
SMPAi.outa24	Seepage results for permeability realization #4
SMPAi.outa25	Seepage results for permeability realization #5
SMPAi.outa26	Seepage results for permeability realization #6
SMPAi.outa27	Seepage results for permeability realization #7
SMPAi.outa28	Seepage results for permeability realization #8
SMPAi.outa29	Seepage results for permeability realization #9
SMPAi.outa210	Seepage results for permeability realization #10

k1-10_realizations_10-scenarios/Sensitivity_analysis_4-scenarios/Logk_Stdev/stdev=0.5/Input/

SMPAsd5.mes1	Mesh with permeability realization #1
SMPAsd5.mes2	Mesh with permeability realization #2
SMPAsd5.mes3	Mesh with permeability realization #3
SMPAsd5.mes4	Mesh with permeability realization #4
SMPAsd5.mes5	Mesh with permeability realization #5
SMPAsd5.mes6	Mesh with permeability realization #6
SMPAsd5.mes7	Mesh with permeability realization #7
SMPAsd5.mes8	Mesh with permeability realization #8
SMPAsd5.mes9	Mesh with permeability realization #9
SMPAsd5.mes10	Mesh with permeability realization #10
Permsd5.par	SISIM input file to generate heterogeneous log-permeability modifier field
sh.meshsd5	Sequence of commands used to generate meshes for 10 realizations

k1-10_realizations_10-scenarios/Sensitivity_analysis_4-scenarios/Logk_Stdev/stdev=0.5/Output/

SMPAi.outsd51	Seepage results for permeability realization #1
SMPAi.outsd52	Seepage results for permeability realization #2
SMPAi.outsd53	Seepage results for permeability realization #3
SMPAi.outsd54	Seepage results for permeability realization #4
SMPAi.outsd55	Seepage results for permeability realization #5
SMPAi.outsd56	Seepage results for permeability realization #6
SMPAi.outsd57	Seepage results for permeability realization #7
SMPAi.outsd58	Seepage results for permeability realization #8
SMPAi.outsd59	Seepage results for permeability realization #9
SMPAi.outsd510	Seepage results for permeability realization #10

k1-10_realizations_10-scenarios/Sensitivity_analysis_4-scenarios/Logk_Stdev/stdev=2.0/Input/

SMPAs2.mes1	Mesh with permeability realization #1
SMPAs2.mes2	Mesh with permeability realization #2
SMPAs2.mes3	Mesh with permeability realization #3
SMPAs2.mes4	Mesh with permeability realization #4
SMPAs2.mes5	Mesh with permeability realization #5
SMPAs2.mes6	Mesh with permeability realization #6
SMPAs2.mes7	Mesh with permeability realization #7
SMPAs2.mes8	Mesh with permeability realization #8
SMPAs2.mes9	Mesh with permeability realization #9
SMPAs2.mes10	Mesh with permeability realization #10
Perms2.par	SISIM input file to generate heterogeneous log-permeability modifier field
sh.meshs2	Sequence of commands used to generate meshes for 10 realizations

k1-10_realizations_10-scenarios/Sensitivity_analysis_4-scenarios/
Logk_Stdev/stdev=2.0/Output/

SMPAi.outs21	Seepage results for permeability realization #1
SMPAi.outs22	Seepage results for permeability realization #2
SMPAi.outs23	Seepage results for permeability realization #3
SMPAi.outs24	Seepage results for permeability realization #4
SMPAi.outs25	Seepage results for permeability realization #5
SMPAi.outs26	Seepage results for permeability realization #6
SMPAi.outs27	Seepage results for permeability realization #7
SMPAi.outs28	Seepage results for permeability realization #8
SMPAi.outs29	Seepage results for permeability realization #9
SMPAi.outs210	Seepage results for permeability realization #10

(Related to section 6.6.3)
k1-10_realizations_10-scenarios/k1-10_realizations_6-scenarios/
k1-10_realizations_10-scenarios/k1-10_realizations_6-scenarios/
Common_input/

SMPA	TOUGH2 input file

k1-10_realizations_10-scenarios/k1-10_realizations_6-scenarios/
Common_input/75+wst_inputs/

Perm.par	SISIM input file to generate heterogeneous log-permeability modifier field

k1-10_realizations_10-scenarios/k1-10_realizations_6-scenarios/
Common_input/Tptpll_inputs/

parametersetrfll.dat	Input file of parameter combination for Tptpll

k1-10_realizations_10-scenarios/k1-10_realizations_6-scenarios/
Common_input/Tptpmn_inputs/

parametersetrfmn.dat	Input file of parameter combination for Tptpmn

k1-10_realizations_10-scenarios/k1-10_realizations_6-scenarios/
Common_input/base_case_inputs/

SMPA.mes1	Mesh with permeability realization #1
SMPA.mes2	Mesh with permeability realization #2
SMPA.mes3	Mesh with permeability realization #3
SMPA.mes4	Mesh with permeability realization #4
SMPA.mes5	Mesh with permeability realization #5
SMPA.mes6	Mesh with permeability realization #6
SMPA.mes7	Mesh with permeability realization #7
SMPA.mes8	Mesh with permeability realization #8
SMPA.mes9	Mesh with permeability realization #9
SMPA.mes10	Mesh with permeability realization #10

k1-10_realizations_10-scenarios/k1-10_realizations_6-scenarios/
Tptpll_75percentile_case/Input/

SMPAll75.mes1	Mesh with permeability realization #1
SMPAll75.mes2	Mesh with permeability realization #2
SMPAll75.mes3	Mesh with permeability realization #3
SMPAll75.mes4	Mesh with permeability realization #4
SMPAll75.mes5	Mesh with permeability realization #5
SMPAll75.mes6	Mesh with permeability realization #6
SMPAll75.mes7	Mesh with permeability realization #7
SMPAll75.mes8	Mesh with permeability realization #8
SMPAll75.mes9	Mesh with permeability realization #9
SMPAll75.mes10	Mesh with permeability realization #10
SMPAll75cut.mes	Mesh file with 75 percentile case of the rock fall in Tptpll
sh.meshll75	Sequence of commands used to generate meshes for 10 realizations

k1-10_realizations_10-scenarios/k1-10_realizations_6-scenarios/
Tptpll_75percentile_case/Output/

SMPAi.outll751	Seepage results for permeability realization #1
SMPAi.outll752	Seepage results for permeability realization #2
SMPAi.outll753	Seepage results for permeability realization #3
SMPAi.outll754	Seepage results for permeability realization #4
SMPAi.outll755	Seepage results for permeability realization #5
SMPAi.outll756	Seepage results for permeability realization #6
SMPAi.outll757	Seepage results for permeability realization #7
SMPAi.outll758	Seepage results for permeability realization #8
SMPAi.outll759	Seepage results for permeability realization #9
SMPAi.outll7510	Seepage results for permeability realization #10
SMPAioutll75.dat	Data file with processed seepage results from 10 realizations

k1-10_realizations_10-scenarios/k1-10_realizations_6-scenarios/
Tptpll_base_case/Input/

SMPAill	iTOUGH2 input file for Tptpll

k1-10_realizations_10-scenarios/k1-10_realizations_6-scenarios/
Tptpll_base_case/Output/

SMPAi.outllb1	Seepage results for permeability realization #1
SMPAi.outllb2	Seepage results for permeability realization #2
SMPAi.outllb3	Seepage results for permeability realization #3
SMPAi.outllb4	Seepage results for permeability realization #4
SMPAi.outllb5	Seepage results for permeability realization #5
SMPAi.outllb6	Seepage results for permeability realization #6
SMPAi.outllb7	Seepage results for permeability realization #7
SMPAi.outllb8	Seepage results for permeability realization #8
SMPAi.outllb9	Seepage results for permeability realization #9
SMPAi.outllb10	Seepage results for permeability realization #10
SMPAioutllb.dat	Data file with processed seepage results from 10 realizations

k1-10_realizations_10-scenarios/k1-10_realizations_6-scenarios/
Tptpll_worst_case/Intput/

SMPAllw.mes1	Mesh with permeability realization #1
SMPAllw.mes2	Mesh with permeability realization #2
SMPAllw.mes3	Mesh with permeability realization #3
SMPAllw.mes4	Mesh with permeability realization #4
SMPAllw.mes5	Mesh with permeability realization #5
SMPAllw.mes6	Mesh with permeability realization #6
SMPAllw.mes7	Mesh with permeability realization #7
SMPAllw.mes8	Mesh with permeability realization #8
SMPAllw.mes9	Mesh with permeability realization #9
SMPAllw.mes10	Mesh with permeability realization #10
SMPAllwcut.mes	Mesh file with worse case of the rock fall in Tptpll
sh.meshllws	Sequence of commands used to generate meshes for 10 realizations

k1-10_realizations_10-scenarios/k1-10_realizations_6-scenarios/
Tptpll_worst_case/Output/

SMPAi.outllw1	Seepage results for permeability realization #1
SMPAi.outllw2	Seepage results for permeability realization #2
SMPAi.outllw3	Seepage results for permeability realization #3
SMPAi.outllw4	Seepage results for permeability realization #4
SMPAi.outllw5	Seepage results for permeability realization #5
SMPAi.outllw6	Seepage results for permeability realization #6
SMPAi.outllw7	Seepage results for permeability realization #7
SMPAi.outllw8	Seepage results for permeability realization #8
SMPAi.outllw9	Seepage results for permeability realization #9
SMPAi.outllw10	Seepage results for permeability realization #10
SMPAioutllw.dat	Data file with processed seepage results from 10 realizations

k1-10_realizations_10-scenarios/k1-10_realizations_6-scenarios/
Tptpmn_75percentile_case/Input/

SMPAmn75.mes1	Mesh with permeability realization #1
SMPAmn75.mes2	Mesh with permeability realization #2
SMPAmn75.mes3	Mesh with permeability realization #3
SMPAmn75.mes4	Mesh with permeability realization #4
SMPAmn75.mes5	Mesh with permeability realization #5
SMPAmn75.mes6	Mesh with permeability realization #6
SMPAmn75.mes7	Mesh with permeability realization #7
SMPAmn75.mes8	Mesh with permeability realization #8
SMPAmn75.mes9	Mesh with permeability realization #9
SMPAmn75.mes10	Mesh with permeability realization #10
SMPAmn75cut.mes	Mesh file with 75 percentile case of the rock fall in Tptpmn
sh.meshmn75s	Sequence of commands used to generate meshes for 10 realizations

k1-10_realizations_10-scenarios/k1-10_realizations_6-scenarios/
Tptpmn_75percentile_case/Output/

SMPAi.outmn751	Seepage results for permeability realization #1
SMPAi.outmn752	Seepage results for permeability realization #2
SMPAi.outmn753	Seepage results for permeability realization #3
SMPAi.outmn754	Seepage results for permeability realization #4
SMPAi.outmn755	Seepage results for permeability realization #5
SMPAi.outmn756	Seepage results for permeability realization #6
SMPAi.outmn757	Seepage results for permeability realization #7
SMPAi.outmn758	Seepage results for permeability realization #8
SMPAi.outmn759	Seepage results for permeability realization #9
SMPAi.outmn7510	Seepage results for permeability realization #10
SMPAioutmn75.dat	Data file with processed seepage results from 10 realizations

k1-10_realizations_10-scenarios/k1-10_realizations_6-scenarios/
Tptpmn_base_case/Input/

SMPAimn	iTOUGH2 input file for Tptpmn base case

k1-10_realizations_10-scenarios/k1-10_realizations_6-scenarios/
Tptpmn_base_case/Output/

SMPAi.outmnb1	Seepage results for permeability realization #1
SMPAi.outmnb2	Seepage results for permeability realization #2
SMPAi.outmnb3	Seepage results for permeability realization #3
SMPAi.outmnb4	Seepage results for permeability realization #4
SMPAi.outmnb5	Seepage results for permeability realization #5
SMPAi.outmnb6	Seepage results for permeability realization #6
SMPAi.outmnb7	Seepage results for permeability realization #7
SMPAi.outmnb8	Seepage results for permeability realization #8
SMPAi.outmnb9	Seepage results for permeability realization #9
SMPAi.outmnb10	Seepage results for permeability realization #10
SMPAioutmnb.dat	Data file with processed seepage results from 10 realizations

k1-10_realizations_10-scenarios/k1-10_realizations_6-scenarios/
Tptpmn_worst_case/Input/

SMPAmnw.mes1	Mesh with permeability realization #1
SMPAmnw.mes2	Mesh with permeability realization #2
SMPAmnw.mes3	Mesh with permeability realization #3
SMPAmnw.mes4	Mesh with permeability realization #4
SMPAmnw.mes5	Mesh with permeability realization #5
SMPAmnw.mes6	Mesh with permeability realization #6
SMPAmnw.mes7	Mesh with permeability realization #7
SMPAmnw.mes8	Mesh with permeability realization #8
SMPAmnw.mes9	Mesh with permeability realization #9
SMPAmnw.mes10	Mesh with permeability realization #10
SMPAmnwcut.mes	Mesh file with worse case of the rock fall in Tptpmn
sh.meshmnws	Sequence of commands used to generate meshes for 10 realizations

k1-10_realizations_10-scenarios/k1-10_realizations_6-scenarios/
Tptpmn_worst_case/Output/

SMPAi.outmnw1	Seepage results for permeability realization #1
SMPAi.outmnw2	Seepage results for permeability realization #2
SMPAi.outmnw3	Seepage results for permeability realization #3
SMPAi.outmnw4	Seepage results for permeability realization #4
SMPAi.outmnw5	Seepage results for permeability realization #5
SMPAi.outmnw6	Seepage results for permeability realization #6
SMPAi.outmnw7	Seepage results for permeability realization #7
SMPAi.outmnw8	Seepage results for permeability realization #8
SMPAi.outmnw9	Seepage results for permeability realization #9
SMPAi.outmnw10	Seepage results for permeability realization #10
SMPAioutmnw.dat	Data file with processed seepage results from 10 realizations

(Related to Section 6.6.3 – Saturation Distribution)

k1-r_6-s_moisture-mapping/

k1-r_6-s_moisture-mapping/T2_input/

SMPA	TOUGH2 input file
SMPA.mes1	Mesh with permeability realization #1 for base case
SMPAll75.mes1	Mesh with permeability realization #1 for 75 percentile case in Tptpll
SMPAllw.mes1	Mesh with permeability realization #1 for the worse case in Tptpll
SMPAmn75.mes1	Mesh with permeability realization #1 for 75 percentile case in Tptpmn
SMPAmnw.mes1	Mesh with permeability realization #1 for the worse case in Tptpll
parametersetrfll.dat	Data file of parameter combination for Tptpll
parametersetrfmn.dat	Data file of parameter combination for Tptpmn

k1-r_6-s_moisture-mapping/T2_output/

SMPA.ll1s	TOUGH2 output file for the base case in Tptpll
SMPA.ll751s	TOUGH2 output file for 75 percentile case in Tptpll
SMPA.llw1s	TOUGH2 output file for the worse case in Tptpll
SMPA.mn1s	TOUGH2 output file for the base case in Tptpmn
SMPA.mn751s	TOUGH2 output file for 75 percentile case in Tptpmn
SMPA.mnw1s	TOUGH2 output file for the worse case in Tptpmn

k1-r_6-s_moisture-mapping/iT2_input/

SMPAill	iTOUGH2 input file for the base case in Tptpll
SMPAill75	iTOUGH2 input file for 75 percentile case in Tptpll
SMPAillw	iTOUGH2 input file for the worse case in Tptpll
SMPAimn	iTOUGH2 input file for the base case in Tptpmn
SMPAimn75	iTOUGH2 input file for 75 percentile case in Tptpmn
SMPAimnw	iTOUGH2 input file for the worse case in Tptpmn

k1-r_6-s_moisture-mapping/iT2_output/

SMPAi.outll1s	TOUGH2 output file for the base case in Tptpll
SMPAi.outll751s	iTOUGH2 output file for 75 percentile case in Tptpll
SMPAi.outllw1s	iTOUGH2 output file for the worse case in Tptpll
SMPAi.outmn1s	iTOUGH2 output file for the base case in Tptpmn
SMPAi.outmn751s	iTOUGH2 output file for 75 percentile case in Tptpmn
SMPAi.outmnw1s	iTOUGH2 output file for the worse case in Tptpmn

Table I-2 lists the plot files and tables in this Model Report. The .wmf files produced by TecPlot can be viewed by opening MS Word 97 (or newer), going to the pull-down menu for Insert → Picture, and then choosing the desired figure file.

Table I-2. File for Figures and Tables in This Model Report **DTN: LB0304SMDCREV2.002**

File name	Folder
fig6-1.wmf	\Completed image files
fig6-10.wmf	\Completed image files
fig6-11.wmf	\Completed image files
fig6-12.wmf	\Completed image files
fig6-13.wmf	\Completed image files
fig6-14a.wmf	\Completed image files
fig6-14b.wmf	\Completed image files
fig6-15.wmf	\Completed image files
fig6-16a.wmf	\Completed image files
fig6-16b.wmf	\Completed image files
fig6-17.wmf	\Completed image files
fig6-18a.wmf	\Completed image files
fig6-18b.wmf	\Completed image files
fig6-19.wmf	\Completed image files
fig6-20a.wmf	\Completed image files
fig6-20b.wmf	\Completed image files
fig6-21.wmf	\Completed image files
fig6-3.wmf	\Completed image files
fig6-4a.wmf	\Completed image files
fig6-4b.wmf	\Completed image files
fig6-5.wmf	\Completed image files
fig6-6.wmf	\Completed image files
fig6-7.wmf	\Completed image files
fig6-8.wmf	\Completed image files
fig6-9.wmf	\Completed image files
fig_llbmean.xls	\Supporting data for tecplot input
fig_mnbmean.xls	\Supporting data for tecplot input
fig6-10.txt	\Supporting data for tecplot input
fig6-10_1.xls	\Supporting data for tecplot input
fig6-10_2.xls	\Supporting data for tecplot input
fig6-11.txt	\Supporting data for tecplot input
fig6-11_1.xls	\Supporting data for tecplot input
fig6-11_2.xls	\Supporting data for tecplot input
fig6-12.txt	\Supporting data for tecplot input
fig6-12.xls	\Supporting data for tecplot input
fig6-13.txt	\Supporting data for tecplot input
fig6-13.xls	\Supporting data for tecplot input
fig6-15.txt	\Supporting data for tecplot input
fig6-15.xls	\Supporting data for tecplot input
fig6-15_1.xls	\Supporting data for tecplot input

Table I-2. File for Figures and Tables in This Model Report **DTN: LB0304SMDCREV2.002 (Continued)**

Fig6-15_2.xls	\Supporting data for tecplot input
fig6-17.txt	\Supporting data for tecplot input
fig6-17.xls	\Supporting data for tecplot input
fig6-17_1.xls	\Supporting data for tecplot input
fig6-17_2.xls	\Supporting data for tecplot input
fig6-19.txt	\Supporting data for tecplot input
fig6-19.xls	\Supporting data for tecplot input
fig6-19_1.xls	\Supporting data for tecplot input
fig6-19_2.xls	\Supporting data for tecplot input
fig6-2.doc	\Supporting data for tecplot input
fig6-21.txt	\Supporting data for tecplot input
fig6-21.xls	\Supporting data for tecplot input
fig6-21_1.xls	\Supporting data for tecplot input
fig6-21_2.xls	\Supporting data for tecplot input
fig6-3.txt	\Supporting data for tecplot input
Fig6-35to6-8.dat	\Supporting data for tecplot input
Fig6-3to6-8.xls	\Supporting data for tecplot input
fig6-9.txt	\Supporting data for tecplot input
fig6-9_1.xls	\Supporting data for tecplot input
fig6-9_2.xls	\Supporting data for tecplot input
readme-fig3to8	Readme file for figures 3 to 8
Table7-1.xls	\Supporting data for tecplot input

Table I-3 lists computer files to simulate the impact of thermal-hydrological-mechanical effects on seepage (Section 6.7). The simulation result is used to compare seepage rates immediately after excavation and 10,000 years after spent fuel emplacement.

Table I-3. Files for the impact of Thermal-Hydrologic-Mechanical Effects on Seepage
DTN: LB0304SMDCREV2.003

File name	Folder
incon	TOUGH2 input file
SVPARAM.DAT	
Hmdelb_10ky	\10ky
Tmn1_mh_1200mm_10ky_5cm.dat	\10ky
Tmn1_mh_1200mm_10ky_5cm.out	\10ky
Tmn1_mh_120mm_10ky_5cm.dat	\10ky
Tmn1_mh_120mm_10ky_5cm.out	\10ky
Tmn1_mh_1800mm_10ky.dat	\10ky
Tmn1_mh_1800mm_10ky.out	\10ky
Tmn1_mh_2400mm_10ky_5cm.dat	\10ky
Tmn1_mh_2400mm_10ky_5cm.out	\10ky
Tmn1_mh_240mm_10ky_5cm.dat	\10ky
Tmn1_mh_240mm_10ky_5cm.out	\10ky
Tmn1_mh_360mm_10ky_5cm.dat	\10ky
Tmn1_mh_360mm_10ky_5cm.out	\10ky
Tmn1_mh_6000mm_10ky.dat	\10ky
Tmn1_mh_6000mm_10ky.out	\10ky
Tmn1_mh_600mm_10ky_5cm.dat	\10ky
Tmn1_mh_600mm_10ky_5cm.out	\10ky
Tmn1_mh_60mm_10ky_5cm.dat	\10ky
Tmn1_mh_60mm_10ky_5cm.out	\10ky
Hmdelb_001y_excavation	\post-excavation
Tmn1_mh_1200mm_exc_5cm.dat	\post-excavation
Tmn1_mh_1200mm_exc_5cm.out	\post-excavation
Tmn1_mh_120mm_exc_5cm.dat	\post-excavation
Tmn1_mh_120mm_exc_5cm.out	\post-excavation
Tmn1_mh_1800mm_exc_5cm.dat	\post-excavation
Tmn1_mh_1800mm_exc_5cm.out	\post-excavation
Tmn1_mh_2400mm_exc_5cm.dat	\post-excavation
Tmn1_mh_2400mm_exc_5cm.out	\post-excavation
Tmn1_mh_240mm_exc_5cm.dat	\post-excavation
Tmn1_mh_240mm_exc_5cm.out	\post-excavation
Tmn1_mh_360mm_exc_5cm.dat	\post-excavation
Tmn1_mh_360mm_exc_5cm.out	\post-excavation
Tmn1_mh_6000mm_exc_5cm.dat	\post-excavation
Tmn1_mh_6000mm_exc_5cm.out	\post-excavation
Tmn1_mh_600mm_exc_5cm.dat	\post-excavation
Tmn1_mh_600mm_exc_5cm.out	\post-excavation
Tmn1_mh_60mm_exc_5cm.dat	\post-excavation
Tmn1_mh_60mm_exc_5cm.out	\post-excavation

Below gives the plot file in this Model Report and support data files for the impact of Thermal-Hydrologic-Mechanical effects on seepage. The .wmf files produced by TecPlot can be viewed by opening MS Word 97 (or newer), going to the pull-down menu for Insert → Picture, and then choosing the desired figure file.

Table I-4. Files for plotting results of the impact of Thermal-Hydrologic-Mechanical Effects on Seepage; DTN: LB0304SMDCREV2.004

Fig6-22.tec	Tecplot file
Fig6-22.wmf	Image file
Fig6-22.xls	Microsoft Excel file

ATTACHMENT II—DATA REDUCTION STEPS FOR ResponseSurfaceSMPA.dat

Section 6.6.1 discusses the seepage results. The seepage percentage is defined as the ratio of the seepage rate into a drift section to the percolation rate applied to the top of the model over the projected cross-sectional area of that drift section. The seepage rate for model calculation is transformed to response surface of seepage into drift in kilograms of water per year per waste package (kg/yr/wp) of 5.5 m diameter and 5.1 m length (design drawings 800-IED-EBS0-00200-000-00A (BSC 2002 [160798]) and 800-IED-EBS0-00100-000-00A (BSC 2002 [160317])). The data reductions were performed using standard functions of the exempt software EXCEL (2000 SR-1). Detailed simulation results for all 20 realizations with every combination of k_{FC}, $1/\alpha$, and Q_p values were submitted to TDMS (Output-DTN: LB0304SMDCREV2.002). The following steps explain the data reduction to obtain ResponseSurfaceSMPA.dat.

Steps:

1 In SMPAi.out*, delete all lines containing word "MESSAGE" and the empty line that follows it

2 Copy SMPAi.out to ResponseSurfaceSMPA.dat

3 Remove all lines with "MESSAGE" and surrounding empty lines

4 Remove lines 1-227 and 2778-end of file; remove columns 5 and 6

5 Copy column 5 between lines 228 and 2777 from files SMPAi.out2 to SMPAi.out20 and add as column 5-23 to file ResponseSurfaceSMPA.dat

6 Open file ResponseSurfaceSMPA.dat in EXCEL and sort rows according to first three columns

7 Insert new columns 4-7; column 1 is log(k), column 2 is 1/alpha, column 3 is percolation flux, columns 8-27 are the seep flow rates for 20 realizations; In file SMPAi, an adjustment factor of 10 should be imposed as part of unit conversion

8 Column 4 = (average of columns 8-27)*10; this is the average seepage flux (kg/year/wp); the adjustment factor of 10 is multiplied to results

9 Column 5 = (std. dev. of columns 8-27)*10; this is the standard deviation of the seepage flux

10 Column 6 = column 4 / (5.5*5.1*column 3) * 100; this is the average seepage percentage

11 Column 7 = column 5 / (5.5*5.1*column 3) * 100; this is the seepage percentage standard deviation

12 Save Columns 1-7 as formatted text file to ResponseSurfaceSMPA.prn

13 Copy ResponseSurfaceSMPA.prn to ResponseSurfaceSMPA.dat

14 Replace results from runs with convergence failure with a seepage percentage of 100% and std. dev. of 14%

15 Add following header for Tecplot plotting:

16 variables = "log(k [m^2]" "1/`a [Pa]" "Percolation [mm/yr]" "Mean Seepage [kg/yr/wp]" "Std. Dev. Seepage [kg/yr/wp]" "Mean Seepage [%]" "Std. Dev. Seepage [%]"

17 ZONE i=15 j=10 k=17

Table II-1. Portion of the EXCEL spreadsheet ResponseSurfaceSMPA.dat

log(k [m^2])	1/alpha [Pa]	Q [mm/yr]	Mean Seepage [kg/yr/WP]	Std. Dev. Seepage [kg/yr/WP]	Mean Seepage [%]	Std. Dev. Seepage [%]
–14.00	100.00	1.00	27.73	4.09	98.86	14.59
–14.00	100.00	5.00	138.92	20.55	99.05	14.65
–14.00	100.00	10.00	277.90	41.19	99.07	14.68
–14.00	100.00	20.00	555.87	82.54	99.09	14.71
–14.00	100.00	50.00	1391.67	205.57	99.23	14.66
–14.00	100.00	100.00	2793.55	406.70	99.59	14.50
–14.00	100.00	200.00	5647.67	785.46	100.67	14.00
–14.00	100.00	300.00	8549.04	1138.98	101.59	13.54
–14.00	100.00	400.00	11501.48	1444.29	102.51	12.87
–14.00	100.00	500.00	14438.54	1717.99	102.95	12.25
–14.00	100.00	600.00	17465.25	2000.48	103.77	11.89
–14.00	100.00	700.00	20002.63	3090.90	101.87	15.74
–14.00	100.00	800.00	23071.27	2838.05	102.81	12.65
–14.00	100.00	900.00	25411.46	3312.18	100.66	13.12
–14.00	100.00	1000.00	27391.33	4644.34	97.65	16.56
–14.00	200.00	1.00	26.14	4.21	93.21	15.00
–14.00	200.00	5.00	136.40	20.51	97.26	14.62
–14.00	200.00	10.00	275.20	40.73	98.11	14.52
–14.00	200.00	20.00	553.39	81.32	98.64	14.49
–14.00	200.00	50.00	1390.78	201.98	99.16	14.40
–14.00	200.00	100.00	2791.65	395.09	99.52	14.09
–14.00	200.00	200.00	5640.64	772.08	100.55	13.76
–14.00	200.00	300.00	8535.17	1112.75	101.43	13.22
–14.00	200.00	400.00	11470.97	1423.23	102.24	12.68
–14.00	200.00	500.00	14390.11	1766.79	102.60	12.60
–14.00	200.00	600.00	16614.64	3155.42	98.72	18.75
–14.00	200.00	700.00	18537.22	4460.73	94.41	22.72
–14.00	200.00	800.00	19405.12	5588.98	86.48	24.91
–14.00	200.00	900.00	20536.87	5452.22	81.35	21.60

ATTACHMENT III—DATA REDUCTION STEPS FOR FIGURE 6-9 TO 6-11

Figures 6-9 to 6-11 discuss the seepage results in the form of seepage percentage. The seepage percentage is defined as the ratio of the seepage rate into a drift section to the percolation rate applied to the top of the model over the projected cross-sectional area of that drift section. It corresponds to simulated total seepage rates into a drift of 5.5 m diameter and 5.1 m length (design drawings 800-IED-EBS0-00200-000-00A (BSC 2002 [160798]) and 800-IED-EBS0-00100-000-00A (BSC 2002 [160317])). The data reductions were performed using standard functions of the exempt software EXCEL (2000 SR-1). Detailed simulation results were submitted to TDMS (Output-DTN: LB0304SMDCREV2.002). The following steps explain the data reduction for seepage results, using worksheets fig6-10_1.xls and fig6-10_2.xls as examples.

Steps:

1 Generate a new file qq* from SMPAi.out* by using command " grep "-0.1200000E+02 0.5000000E+03" SMPAi.out* > qq*"

2 Copy qq* to qqq.dat

3 Open file qqq.dat and save as fig6-10_1 in EXCEL and delete columns A, B, E and F

4 Insert new column 2; column 1 is log(k), column 3 is the seepage flow rate

5 Insert new row 1 and add header

6 Column 2 = column 2 *10 / (5.5*5.1* 200) * 100; this is the seepage percentage; the factor of 10 1s an adjustment factor for unit conversion and 200 is the percolation flux

7 Save fig6-10_1 as formatted text file

8 Open EXCEL file fig6-10_1 and save as fig6-10_2 in EXCEL

9 Copy rows C17 to C31 as D2 to D16; C32 to C46 as E2 to E16; … C287 to C301 as V2 to V16; columns C to V are 20 realizations

10 Column 2 = (average of columns C-V)*10 / (5.5*5.1*200) * 100; this is the average seepage percentage

11 Save fig6-10_2 as formatted text file

12 Keep columns 1 and 2 in the text files fig6-10_1 and fig6-10_2 and save together as a fig6-10 for Tecplot plotting

Table III-1. Portion of the EXCEL Spreadsheet fig6-10_1

Qp(mm/yr)	Seep.(%)	Real.
1.00E+00	0.00	1.00E-50
5.00E+00	0.00	1.00E-50
1.00E+01	0.16	4.60E-02
2.00E+01	5.44	3.05E+00
5.00E+01	31.65	4.44E+01
1.00E+02	42.98	1.21E+02
2.00E+02	50.59	2.84E+02
3.00E+02	54.40	4.58E+02
4.00E+02	56.90	6.38E+02
5.00E+02	58.78	8.24E+02
6.00E+02	60.13	1.01E+03
7.00E+02	61.25	1.20E+03
8.00E+02	62.12	1.39E+03
9.00E+02	62.90	1.59E+03
1.00E+03	63.59	1.78E+03
1.00E+00	0.00	1.00E-50
5.00E+00	0.00	1.00E-50
1.00E+01	0.01	4.08E-03
2.00E+01	19.01	1.07E+01
5.00E+01	50.01	7.01E+01
1.00E+02	73.56	2.06E+02
2.00E+02	87.52	4.91E+02
3.00E+02	92.69	7.80E+02
4.00E+02	96.09	1.08E+03

Table III-2. Portion of the EXCEL Spreadsheet fig6-10_2

Qp(mm/yr)	Mean Seep. (%)	Real.1	Real. 2	Real. 3	Real. 4	Real. 5	Real. 6	Real. 7
1.00E+00	0.00	1.00E-50	1.00E-50	1.00E-50	1.00E-50	1.00E-50	1.00E-50	1.00E-50
5.00E+00	0.22	1.00E-50	1.00E-50	1.00E-50	1.00E-50	1.00E-50	1.00E-50	1.00E-50
1.00E+01	3.82	4.60E-02	4.08E-03	9.06E-02	7.41E-02	6.82E-01	1.00E-50	3.81E-01
2.00E+01	14.55	3.05E+00	1.07E+01	6.66E+00	2.93E+00	1.28E+01	5.24E+00	3.50E+00
5.00E+01	38.09	4.44E+01	7.01E+01	4.99E+01	6.60E+01	7.29E+01	4.56E+01	3.31E+01
1.00E+02	55.27	1.21E+02	2.06E+02	1.50E+02	2.01E+02	1.94E+02	1.45E+02	1.22E+02
2.00E+02	68.65	2.84E+02	4.91E+02	3.69E+02	4.83E+02	4.45E+02	3.79E+02	3.54E+02
3.00E+02	74.55	4.58E+02	7.80E+02	5.97E+02	7.68E+02	7.00E+02	6.20E+02	5.95E+02
4.00E+02	78.19	6.38E+02	1.08E+03	8.28E+02	1.06E+03	9.73E+02	8.68E+02	8.44E+02
5.00E+02	80.63	8.24E+02	1.38E+03	1.06E+03	1.36E+03	1.25E+03	1.12E+03	1.10E+03
6.00E+02	82.39	1.01E+03	1.68E+03	1.30E+03	1.66E+03	1.53E+03	1.37E+03	1.36E+03
7.00E+02	83.75	1.20E+03	1.98E+03	1.54E+03	1.96E+03	1.81E+03	1.62E+03	1.62E+03
8.00E+02	98.86	1.39E+03	2.29E+03	1.78E+03	2.26E+03	2.10E+03	1.87E+03	1.88E+03
9.00E+02	85.74	1.59E+03	2.59E+03	2.02E+03	2.57E+03	2.38E+03	2.13E+03	2.14E+03
1.00E+03	86.51	1.78E+03	2.89E+03	2.25E+03	2.88E+03	2.67E+03	2.38E+03	2.40E+03

ATTACHMENT IV—DATA REDUCTION STEPS FOR FIGURES OF ROCK FALL

Section 6.6.3 discusses the seepage results of rock fall. The seepage percentage is defined as the ratio of the seepage rate into a drift section to the percolation rate applied to the top of the model over the projected cross-sectional area of that drift section. It corresponds to simulated total seepage rates into a drift of 5.5 m diameter and 5.1 m length (design drawings 800-IED-EBS0-00200-000-00A (BSC 2002 [160798]) and 800-IED-EBS0-00100-000-00A (BSC 2002 [160317])). The data reductions were performed using standard functions of the exempt software EXCEL (2000 SR-1). Detailed simulation results were submitted to TDMS (Output-DTN: LB0304SMDCREV2.002). The following steps explain the data reduction for seepage results, using worksheets fig6-17_1.xls and fig6-17_2.xls as examples.

Steps:

1 In SMPAi.outmnw*, delete all lines containing word "MESSAGE" and the empty line that follows it and only keep the seepage results

2 Copy SMPAi.outmnw* to SMPAioutmnw.dat

3 Open file to SMPAioutmnw.dat and save as fig6-17_1 in EXCEL and delete columns 1, 2, 5 and 6

4 Insert new column 2; column 1 is log(k), column 3 is the seepage flow rate

5 Insert row 1 and add header

6 Column 2 = column 3 *10 / (5.5*5.1* 200) * 100; this is the seepage percentage; the factor of 10 1s an adjustment factor for unit conversion and 200 is the percolation flux

7 Save fig6-17_1 as formatted text file

8 Open EXCEL file fig6-17_1 and save as fig6-17_2 in EXCEL

9 Open EXCEL file fig6-17_2 and copy rows C17 to C31 as D2 to D16; C32 to C46 as E2 to E16; … C137 to C151 as L2 to L16; columns C to L are 10 realizations

10 Column 2 = (average of columns C-L)*10 / (5.5*5.1*200) * 100; this is the average seepage percentage

11 Save fig6-17_2 as formatted text file

12 Use above steps to calculate the average seepage percentage for base case on data SMPAimnb.dat and get formatted text file fig_mnbmean

13 Keep columns A and B in the text files fig6-17_1, fig6-17_2, and fig_mnbmean and save together as a fig6-17 for Tecplot plotting

Table IV-1. Portion of the EXCEL Spreadsheet fig6-17_1

Qp(mm/yr)	Seep.(%)	Seep.
1.00E+00	0.00	1.00E-50
5.00E+00	0.00	1.00E-50
1.00E+01	0.00	1.00E-50
2.00E+01	0.00	1.00E-50
5.00E+01	0.00	1.00E-50
1.00E+02	2.19	6.13E+00
2.00E+02	21.69	1.22E+02
3.00E+02	30.40	2.56E+02
4.00E+02	35.33	3.96E+02
5.00E+02	38.62	5.42E+02
6.00E+02	40.93	6.89E+02
7.00E+02	42.93	8.43E+02
8.00E+02	44.66	1.00E+03
9.00E+02	46.08	1.16E+03
1.00E+03	47.27	1.33E+03
1.00E+00	0.00	1.00E-50
5.00E+00	0.00	1.00E-50
1.00E+01	0.00	1.00E-50
2.00E+01	0.00	1.00E-50
5.00E+01	0.00	1.00E-50
1.00E+02	8.54	2.39E+01

Table IV-2. Portion of the EXCEL Spreadsheet fig6-17_2

Qp(mm/yr)	Mean Seep.(%)	Real.1	Real.2	Real.3	Real.4	Real.5	Real.6	Real.7	Real.8
1.00E+00	0.00	1.00E-50	1.00E-50	1.00E-50	1.00E-50	1.00E-50	1.00E-50	1.00E-50	1.00E-50
5.00E+00	0.00	1.00E-50	1.00E-50	1.00E-50	1.00E-50	1.00E-50	1.00E-50	1.00E-50	1.00E-50
1.00E+01	0.00	1.00E-50	1.00E-50	1.00E-50	1.00E-50	1.00E-50	1.00E-50	1.00E-50	1.00E-50
2.00E+01	0.00	1.00E-50	1.00E-50	1.00E-50	1.00E-50	1.00E-50	1.00E-50	1.00E-50	1.00E-50
5.00E+01	2.62	1.00E-50	1.00E-50	6.17E+00	1.00E-50	2.29E+00	1.00E-50	1.00E-50	1.64E+01
1.00E+02	12.59	6.13E+00	2.39E+01	4.72E+01	1.73E+01	7.56E+01	3.11E+01	9.12E+00	7.03E+01
2.00E+02	31.75	1.22E+02	1.88E+02	1.63E+02	1.68E+02	2.34E+02	1.83E+02	1.09E+02	2.20E+02
3.00E+02	41.60	2.56E+02	4.05E+02	3.03E+02	3.66E+02	4.10E+02	3.39E+02	2.36E+02	4.14E+02
4.00E+02	48.09	3.96E+02	6.40E+02	4.66E+02	5.80E+02	6.11E+02	5.05E+02	3.78E+02	6.26E+02
5.00E+02	52.88	5.42E+02	9.03E+02	6.43E+02	8.07E+02	8.24E+02	6.88E+02	5.34E+02	8.46E+02
6.00E+02	56.77	6.89E+02	1.17E+03	8.30E+02	1.05E+03	1.06E+03	8.78E+02	7.05E+02	1.08E+03
7.00E+02	60.05	8.43E+02	1.44E+03	1.03E+03	1.31E+03	1.29E+03	1.08E+03	8.79E+02	1.33E+03
8.00E+02	62.80	1.00E+03	1.72E+03	1.23E+03	1.58E+03	1.53E+03	1.29E+03	1.07E+03	1.59E+03
9.00E+02	65.12	1.16E+03	2.00E+03	1.44E+03	1.86E+03	1.77E+03	1.50E+03	1.29E+03	1.85E+03
1.00E+03	67.12	1.33E+03	2.28E+03	1.65E+03	2.14E+03	2.02E+03	1.72E+03	1.51E+03	2.10E+03